European Journal of Control 85 (2025) 101254

Contents lists available at ScienceDirect

European Journal of Control

journal homepage: www.sciencedirect.com/journal/european-journal-of-control

Exponential synchronization for Markovian jump Lur'e complex networks using sliding mode control: Application to circuit system

Saravanan Shanmugam [a], Premraj Durairaj [b], R. Vadivel [c], Karthikeyan Rajagopal [d,e,*]

[a] Center for Computational Biology, Easwari Engineering College, Chennai 600 089, Tamilnadu, India
[b] Institute of Systems Science and College of Information Science and Engineering, Huaqiao University, 361021, Xiamen, China
[c] Department of Mathematics, Faculty of Science and Technology, Phuket Rajabhat University, Phuket 83000, Thailand
[d] Center for Research, SRM Institute of Science and Technology-Ramapuram, Chennai 600089, Tamil Nadu, India
[e] Center for Research, Easwari Engineering College, Ramapuram, Chennai, Tamilnadu, 600089, India

ARTICLE INFO

Recommended by T. Parisini

Keywords:
Complex dynamical networks
Markovian jumping
Lyapunov–Krasovskii functional
Sliding mode control
Linear matrix inequality

ABSTRACT

This paper deals with the synchronization problem in Markovian jump complex dynamic networks (MJCDNs) with time-varying delays. The network consists of N nodes that switch between different modes according to known Markovian jump parameters. The synchronization of these complex networks is achieved by sliding mode control (SMC) strategies. The study uses a suitable Lyapunov–Krasovskii functional (LKF) to formulate delay-dependent synchronization criteria as linear matrix inequalities, using free weighted matrices generated by the LKF. Furthermore, an integral sliding surface is developed to ensure the exponential stability of MJCDNs, and a controller is synthesized to derive the trajectory of the closed-loop system to the desired sliding surface. Two numerical examples demonstrate the practical application of the derived theoretical results.

1. Introduction

Complex dynamical networks (CDNs) are gaining significant attention in the scientific community due to their wide-ranging applications in areas like biological research, information science, sociology, secure communication, and beyond (Li & Chen, 2006; Lü, Yu, & Chen, 2004; Wang, Wu, & Huang, 2015). Recently, there has been an increased interest in using CDNs to replicate real-world systems, including social networks, food webs, WWW, and electricity grids (Guan, Liu, Feng, & Wang, 2010; Wang, Liu, She, & Zhong, 2017; Wu, Li, & Li, 2019). Given that these systems communicate within the complex network's sophisticated framework, time delays have become an important factor to take into account (Guan et al., 2010; Li & Chen, 2006; Lü et al., 2004; Wang et al., 2017, 2015; Wu et al., 2019). Time delays are extensive in practice, as the speed of information processing is limited and the switching capabilities of amplifiers are limited. Consequently, they often lead to undesirable dynamic behavior, including system instability and performance degradation. To comprehensively analyze and improve the efficiency of complex networks, it is important to understand the impact of time delays. By exploring the significance of time delays, researchers can gain insights that are essential for optimizing network performance and mitigating potential drawbacks. Understanding the intricate interplay between time delays and network dynamics is critical to advancing various technological applications and ensuring their robustness in the real world. This paper explores the intrinsic temporal dynamics of complex systems and its impact on the behavior of CDNs (Shanmugam, Rhaima, & Ghoudi, 2023; Sivaranjani, Rakkiyappan, & Joo, 2018; Zhong & Song, 2023). This research discusses the fundamental temporal dynamics of complex systems and their influence on the behavior of CDNs. It emphasizes the importance of time delays in understanding and improving these complex networks.

With the expanding scope and complexity of dynamical systems, there is a rising interest among researchers to explore CDNs that are characterized by time delays. This growing field of study involves a wide array of research initiatives, including stability analysis (Xu, Zhu, Liu, & Wen, 2023), state estimation techniques (Chen, Zhang, & Yang, 2023), synchronization (Rakkiyappan, Sasirekha, Lakshmanan, & Lim, 2016), and more. Researchers have come to understand that neural networks are susceptible to the influence of switching signals controlled by Markovian chains, while striving to fully comprehend the complex dynamics of these systems (Sivaranjani et al., 2018; Wang, Dong, & Liao, 2016; Yi, Wang, Xiao, & Huang, 2013). The finding has led to a significant change in the direction of research, focusing on the study of neural networks modeled with finite network modes, known as Markov Jumping Neural Networks (MJNNs) (Ali, Yogambigai, Saravanan, & Elakkia, 2019; Mala, Vinodkumar, & Alzabut, 2023). Recently, scholars

* Corresponding author at: Center for Research, SRM Institute of Science and Technology-Ramapuram, Chennai 600089, Tamil Nadu, India.
E-mail address: rkarthiekeyan@gmail.com (K. Rajagopal).

https://doi.org/10.1016/j.ejcon.2025.101254
Received 30 March 2024; Received in revised form 8 May 2025; Accepted 24 May 2025
Available online 23 June 2025

have conducted diverse research exploring MJNNs from various angles. For instance, in the realm of CDNs and MJNNs, Zhong and Song (2023) undertook a stability analysis focusing on non-fragile synchronization control within T-S fuzzy systems. Additionally, (Yi et al., 2013) investigated into the realm of exponential synchronization, particularly concerning Markovian jump parameters and stochastic delays. Furthermore, Ali et al. (2019), Shanmugam, Vadivel, and Gunasekaran (2023), Wang et al. (2016) explored innovative synchronization strategies for stochastic Cohen–Grossberg BAM NNs with time delays, neutral-type BAM neural networks, and finite-time synchronization of Quantized Markovian-jump delayed NNs, respectively. These studies collectively contribute to the broader understanding and advancement of MJNNs, shedding light on their intricate dynamics and potential applications. The inclusion of MJNNs in the analytical framework of investigations on CDNs with time delay is expected to enhance our comprehension of the intricate behaviors displayed by these systems and facilitate the development of more efficient approaches in their design, optimization, and control.

Considerable attention has been concerned to exploring the dynamic characteristics of CDNs, encompassing optimization, coordination, stability, and synchronization. Among these behaviors, synchronization holds particular significance and has garnered extensive discussion in the literature (Zhou & Chen, 2006). The occurrence of synchronization phenomena is prevalent across various real-world systems, including arrays of identical delayed neural networks, biological systems, and information sciences. This underscores the widespread relevance and applicability of synchronization concepts across diverse domains. As researchers investigate deeper into understanding synchronization dynamics, new insights continue to emerge, fueling further investigations and advancements in the field. It offers valuable insights into the methods of coordinating the rhythms of all or some of the systems in these networks, promoting consistent behavior (Ganesan & Annamalai, 2023; Sakthivel, Kwon, & Selvaraj, 2021). Although adjusting system parameters can synchronize a small number of complicated networks, a significant fraction requires the use of external forces, such as controllers, to achieve different types of synchronization. In addition, advancements in research in this area have led to the creation of numerous control systems specifically designed to synchronize complicated networks (Guan et al., 2010; Li & Chen, 2006; Lü et al., 2004; Wang et al., 2015). This encompasses innovative methodologies in Wang et al. (2017), (Guan et al., 2010; Liu, Ho, & Shi, 2015; Wu et al., 2019), and sliding mode control (SMC) in Chen, Niu, and Zou (2013). In this group, SMC works well as a control technique for CDNs because it responds quickly and is not affected by variations in system parameters or external disturbances. The main way that SMC controls systems is by using a discontinuous controller to push system state trajectories as well as to stay in a predefined subspace. This gives the system the characteristics that are wanted, like being stable, able to track, and able to ignore disturbances (Karimi, 2012; Utkin, 1977). A lot of different control methods have been used to get CDNs to work together, but SMC has been one of the best because of its unique benefits. As a result, SMC has been used successfully on many complicated systems. In a recent study (Liu, Ma, Jiang, & Xi, 2016), researchers examined H_∞ stochastic synchronization within a master–slave semi-Markovian switching system. Similarly, in another work (Chen et al., 2013), the focus was on investigating SMC for a specific class of stochastic Markovian jumping systems. Additionally, a recent contribution by Xu et al. (2023) addressed the finite/fixed-time chaotic delayed neural networks utilizing SMC techniques. Addressing the complexities inherent in the derivation process, the present paper introduces a novel sliding mode function tailored to include characteristics specific to CDNs, thereby addressing a critical challenge in synchronization research.

The Lur'e system, which promises to sector-bound constraints and comprises a linear structure in the forward channel and a nonlinear element in the feedback direction, is a focal point in nonlinear research. Previous studies documented in Refs. (Guo, Nian, Zhao, & Duan, 2012; Tang, Park, & Feng, 2018) underscore the intriguing research focus on synchronization within Lur'e systems. Typically, the nonlinear feedback function $f(\cdot)$ is constrained to specific sector conditions. Lur'e systems encompass various classical chaotic systems as demonstrated by prior works (Rakkiyappan, Velmurugan, George, & Selvamani, 2017; Tang, Park, & Zheng, 2018). Achieving perfect stability remains a central concern within Lur'e systems, driving extensive research into synchronization and its applications. For instance, the authors in Li, Liu, Zhu, Zhong, and Cheng (2019) investigated semi-Markovian jump chaotic Lur'e systems employing stochastic synchronization approaches. In Tang, Park, and Zheng (2018) analyzed distributed impulsive synchronization of Lur'e CDNs. The synchronization of CDNs has useful significant attention due to its broad applications in various fields. The authors in Zhong and Song (2023) demonstrated the effectiveness of non-fragile synchronization control in T-S fuzzy Markovian jump CDNs (MJCDNs), highlighting the need for robust control methods. The authors in Shanmugam, Rhaima, and Ghoudi (2023) explored exponential synchronization in networks with hybrid delays and uncertainties, emphasizing the importance of addressing such complexities under specific control parameters. In Sivaranjani et al. (2018) utilized event-triggered approaches for reliable synchronization in semi-Markovian jumping CDNs, showcasing the benefits of using generalized integral inequalities. Additionally, in Rakkiyappan, Latha, and Sivaranjani (2017) investigated the exponential synchronization of Lur'e CDNs using pinning sampled-data control, demonstrating the relevance of advanced synchronization techniques. However, to the best of the author's knowledge, there is a gap in the literature regarding the synchronization of Markovian jump Lur'e CDNs using SMC. Based on the above analysis, it is necessary to explore the advanced synchronization methods for MJCDNs with time-varying delays through SMC strategies and Lyapunov–Krasovskii functionals (LKF). The main contributions of this paper are outlined as follows:

1. This paper investigates the exponential synchronization of Markovian jump phenomena within complex networks, incorporating time-varying delays and intricate interconnections through a Lur'e system structure.
2. We introduce a novel LKF and apply an new integral inequality approach to establish sufficient conditions for synchronization with SMC, expressed as linear matrix inequalities (LMIs).
3. Our criteria utilize free-weighting matrices, enhancing the flexibility and applicability of synchronization conditions. This approach ensures the exponential stability of MJCDNs by developing an integral sliding surface, providing robust stability in the presence of uncertainties.
4. In addition to addressing the synchronization problem for MJCDNs. The effectiveness of our proposed method is demonstrated through practical applications, including a detailed example with the Chua circuit and comparisons with existing methods to validate and showcase the advantages of our approach.

Notation. The following notations are needed in this paper. $\mathbb{R}^+$ is positive real number, $\mathbb{R}^n$ denotes the n-dimensional Euclidean space and the superscript "T" denotes the transpose of a matrix or vector. I denotes the identity matrix with compatible dimensions. For a symmetric block matrix, we use * to denote the terms introduced by symmetry. $X < Y (X > Y)$, where X and Y are both symmetric matrices. Given a complete probability space$(\Omega, \mathcal{F}, \{\mathcal{F}_t\}_{t\geq 0}, \mathcal{P})$ with a filtration $\{\mathcal{F}_t\}_{t\geq 0}$ satisfying the usual conditions (i.e. it is increasing and right continuous while $\mathcal{F}_0$ contains all $\mathcal{P}$-null sets), where Ω is the sample space, $\mathcal{F}$ is the algebra of events and $\mathcal{P}$ is the probability measure defined on $\mathcal{F}$. The notation $A \otimes B$ stands for the Kronecker product of matrices A and B. $\|\cdot\|$ stands for the Euclidean vector norm. $\mathcal{E}$ stands for the mathematical expectation.

2. problem formulation and preliminaries

Consider a right-continuous Markovian chain denoted by $r_t(t \geq 0)$, operating on the probability space $(\Omega, \mathcal{F}, \{\mathcal{F}_t\}_{t\geq 0}, \mathcal{P})$, where it assumes values within the finite space $S = 1, 2, \ldots, m$. The generator matrix $\phi = \phi_{ij\,m\times m}$, as defined in Xing, Yao, Lu, and Li (2015) governs the transitions between states i and j.

The transition probabilities are described by

$$Pr\{r(t+\Delta t) = j \mid r(t) = i\} = \begin{cases} \phi_{ij}\Delta t + o(\Delta t), & if \quad i \neq j, \\ 1 + \phi_{ij}\Delta t + o(\Delta t), & if \quad i = j. \end{cases}$$

These transition probabilities capture the likelihood of transitioning from state i to state j within a small time interval Δt. The generator matrix ϕ encapsulates the dynamics of the Markovian chain, enabling the analysis of its behavior and properties over time.

Where $\Delta t > 0$ and $\lim_{\Delta t\to 0} \frac{0(\Delta t)}{\Delta t} = 0$, $\phi_{ij} \geq 0$ is the transition rate from i to j if $j \neq i$, while $\phi_{ii} = -\sum_{j\neq i} \phi_{ij}$.

Consider the following MJCDNs coupled Lur'e systems with time-varying delays, constituting N identical nodes, where each node represents an n-dimensional dynamical subsystem:

$$\begin{cases} \dot{x}_k(t) &= A_{r_t}x_k(t) + B_{r_t}x_k(t-d(t)) + C_{r_t}f(Dx_k(t)) \\ &\quad + c_1\sum_{l=1}^{N} g_{kl}\Gamma_{1r_t}x_l(t) + c_2\sum_{l=1}^{N} g_{kl}\Gamma_{2r_t}x_l(t-d(t)) + W_{r_t}u_k(t), \\ x_k(t) &= \varphi_k(t), \qquad t \in [-d, 0], \qquad k = 1, 2, \ldots., N, \end{cases} \tag{1}$$

where, $x_k(t)$ denotes the state vector of the kth node, $r_t(t \geq 0)$ represents the continuous-time Markov process governing the mode evolution at time t, and $u_k(t)$ signifies the constant external input vector. A continuous vector-valued function $\varphi_k(t)$ determines the initial conditions. d and μ are non-negative constants, thereby observing that $0 \leq d(t) \leq d$ and $\dot{d}(t) \leq \mu$ hold for a time-varying delay $d(t)$.

Moreover, A_{r_t}, B_{r_t}, and C_{r_t} are matrix functions of the random process $r_t(t \geq 0)$, while Γ_{1r_t} and Γ_{2r_t} denote constant inner-coupling matrices. The function $f(\cdot)$ represents vector-valued nonlinear functions, and c_1 and c_2 signify the non-delayed and delayed coupling strengths, respectively. Additionally, $G = (g_{kl})_{N\times N}$ serves as the outer-coupling matrix, delineating the topological structure of the complex networks. The connections between nodes are captured by the entries of G, where $g_{kl} = g_{lk} = 1$ if there exists a connection between nodes k and l, and $g_{kl} = 0$ otherwise. The row sums of G are zero, ensuring $\sum_{l=1}^{N} g_{kl} = -g_{kk}$ for $k = 1, 2, \ldots, N$.

For each $f_l(\cdot)$, there exist scalars ν_l^+ and ν_l^- such that

$$\nu_l^- \leq \frac{f_l(D_l^T\alpha_1(t)) - f_l(D_l^T\alpha_2(t))}{D_l^T\alpha_1(t) - D_l^T\alpha_2(t)} \leq \nu_l^+, \qquad l = 1, 2, \ldots, n,$$

where $\alpha_1,\ \alpha_2 \in \mathbb{R}^n$, and $\alpha_1 \neq \alpha_2$.

Let $\bar{x}(t)$ be the solution of the target node of Lur'e system

$$\dot{\bar{x}}(t) = A\bar{x}(t) + B\bar{x}(t-d(t)) + Cf(D(\bar{x}(t))). \tag{2}$$

We define the synchronization error as $e_k = x_k(t) - \bar{x}(t)$. By subtracting Eq. (2) from Eq. (1), we obtain the error dynamical network, given by:

$$\begin{cases} \dot{e}_k(t) &= A_{r_t}e_k(t) + B_{r_t}e_k(t-d(t)) + C_{r_t}h(De_k(t)) \\ &\quad + c_1\sum_{l=1}^{N} g_{kl}\Gamma_{1r_t}x_l(t) + c_2\sum_{l=1}^{N} g_{kl}\Gamma_{2r_t}x_l(t-d(t)) + W_{r_t}u_k(t), \\ e_k(t) &= \varphi_k(t), \qquad t \in [-d, 0], \qquad k = 1, 2, \ldots., N, \end{cases} \tag{3}$$

where $h(De_k(\cdot)) = f(D(e_k(\cdot) + \bar{x}(\cdot))) - f(D\bar{x}(\cdot))$. Therefore, based on (3), it can be found that for any $l = 1, 2, \ldots, n$,

$$\nu_l^- \leq \frac{h_l(D_l^Te_l, \bar{x})}{D_l^Te_l} = \frac{f_l(D_l^T(e_l + \bar{x})) - f_l(D_l^T\bar{x})}{D_l^Te_l} \leq \nu_l^+, \qquad D_l^Te_l \neq 0,$$

from the above, one can conclude that for any $l = 1, 2, \ldots, n$

$$\left[h_l(D_le_l, \bar{x}) - \nu_l^+D_l^Te_l\right]\left[h_l(D_le_l, \bar{x}) - \nu_l^-D_l^Te_l\right] \leq 0.$$

For simplicity, we denote $r_t = i$, subsequently, we can represent the synchronization error system (3) in the following manner:

$$\begin{cases} \dot{e}_k(t) &= A_ie_k(t) + B_ie_k(t-d(t)) + C_ih(De_k(t)) \\ &\quad + c_1\sum_{l=1}^{N} g_{kl}\Gamma_{1i}x_l(t) + c_2\sum_{l=1}^{N} g_{kl}\Gamma_{2i}x_l(t-d(t)) + W_iu_k(t), \\ e_k(t) &= \varphi_k(t), \qquad t \in [-d, 0], \qquad (k = 1, 2, \ldots., N). \end{cases} \tag{4}$$

The original synchronization problem can be reformulated as the task of stabilizing the error system (4) through a suitable selection of SMC techniques. The design of the SMC is rooted in variable structure control principles (Utkin, 1977). To initiate this process, we introduce the sliding surface as follows:

$$\begin{aligned} s_k(t, i) = \mathcal{V}_ie_k(t) - \mathcal{V}_i\int_0^t \Big[&(A_i - W_iK_i)e_k(t) + c_1\sum_{l=1}^{N} g_{kl}\Gamma_{1i}e_l(t) \\ &+ B_ie_k(t-d(t)) \\ &+ c_2\sum_{l=1}^{N} g_{kl}\Gamma_{2i}e_l(t-d(t))\Big]\, ds. \end{aligned} \tag{5}$$

The real matrices $\mathcal{V}_i \in \mathbb{R}^{m\times n}$ and $K_i \in \mathbb{R}^{r\times n}$ are to be designed. The matrix $\mathcal{V}_i$ is designed such that $\mathcal{V}_iW_i$ is non-singular. The condition $\dot{s}_k(t, i) = 0$ is crucial for maintaining the state trajectory on the switching surface $s_k(t, i) = 0$. Thus, the equation $\dot{s}_k(t, i) = 0$ (4), we derive the equivalent control as follows:

$$\begin{aligned} s_k(t, i) = \mathcal{V}_ie_k(t) - \mathcal{V}_i\int_0^t \Big[&(A_i - W_iK_i)e_k(s) + c_1\sum_{l=1}^{N} g_{kl}\Gamma_{1i}e_l(s) \\ &+ B_ie_k(s-d(s)) + c_2\sum_{l=1}^{N} g_{kl}\Gamma_{2i}e_l(s-d(s))\Big]\, ds, \end{aligned} \tag{6}$$

$$0 = \mathcal{V}_iW_iK_ie_k(t) + \mathcal{V}_iC_ih(De_k(t)) + \mathcal{V}_iW_iu_k(t), \tag{7}$$

From the (7) for $u_k(t)$, we obtain,

$$u_k(t) = -K_ie_k(t) - \bar{\mathcal{V}}_iC_ih(De_k(t)), \tag{8}$$

where $\bar{\mathcal{V}}_i = (\mathcal{V}_iW_i)^{-1}\mathcal{V}_i$. Substituting (8) into (5), an analysis of the error dynamics in SDC, we have the following:

$$\begin{aligned} \dot{e}_k(t) =&(A_i - W_iK_i)e_k(t) + B_ie_k(t-d(t)) + (C_i - W_i\bar{\mathcal{V}}_iC_i)h(De_k(t)) \\ &+ c_1\sum_{l=1}^{N} g_{kl}\Gamma_{1i}e_l(t) + c_2\sum_{l=1}^{N} g_{kl}\Gamma_{2i}e_l(t-d(t)). \end{aligned} \tag{9}$$

We can represent the system (9) in a concise form as follows:

$$\begin{aligned} \dot{e}(t) =&(I_N \otimes (A_i - W_iK_i))e(t) + (I_N \otimes B_i)e(t-d(t)) \\ &+ (I_N \otimes (C_i - W_i\bar{\mathcal{V}}_iC_i))h(De(t)) \\ &+ c_1(G \otimes \Gamma_{1i})e(t) + c_2(G \otimes \Gamma_{2i}e(t-d(t))). \end{aligned} \tag{10}$$

Definition 2.1 (*Akbari, Sadr, & Kazemy, 2020*)**.** The master system (1) and the slave system (2) can achieve exponential synchronization if there exist positive scalars β and α satisfying the condition:

$$E\left\{\|e(t)\|^2\right\} \leq \beta e^{-\alpha t}\sup_{-d\leq t\leq 0}\{\|e(t)\|^2, \|\dot{e}(t)\|^2\}, \quad \forall t > 0.$$

Definition 2.2 (*Mao, 1999*)**.** A functional $V(x(t), r(t), t > 0) \equiv V(x(t), r)$ is said to be a stochastic positive functional. Its weak infinitesimal operator can be defined as

$$\begin{aligned} &\mathcal{L}(V(x(t), r(t))) \\ &\quad \equiv \lim_{\Delta t\to 0}\frac{1}{\Delta t}[\mathbb{E}\{V(x(t+\Delta t), r(t+\Delta t), t+\Delta t)|x(t), r(t) = i\} - V(x(t), i, t)] \end{aligned} \tag{11}$$

Lemma 2.3 (*Peng, He, Long, & Wu, 2020*)**.** *Given $R \in \mathbb{R}^{n\times n} > 0$, a vector $w : [\alpha, \beta] \to \mathbb{R}^n$, and an auxiliary scalar function $\{f_i(u) \mid u \in [\alpha, \beta], f_0(u) =$*

1} *satisfying*

$$\int_{\alpha}^{\beta} f_i(s)f_j(s)\,ds = 0, \quad (0 \le i, j \le n, i \ne j)$$

with $f_i(s)$ $(i = 1, \dots, n)$ *not identically zero. Then for any matrices* $N_i \in \mathbb{R}^{k\times n}$ $(i = 0, \dots, n)$ *and a vector* $\eta \in \mathbb{R}^k$*, the following inequality holds:*

$$-\int_{\alpha}^{\beta} w^T(s)Rw(s)\,ds \le \eta^T \left\{ \sum_{i=0}^{n} \int_{\alpha}^{\beta} f_i^2(s)\,ds\, N_i R^{-1} N_i^T + Sym\Big(\sum_{i=0}^{n} N_i \varpi_i\Big) \right\} \eta,$$

where $\varpi_i \in \mathbb{R}^{n\times k}$ $(i = 0, \dots, n)$*, and* $\int_{\alpha}^{\beta} f_i(s)w(s)\,ds = \varpi_i \eta$*.*

Lemma 2.4 (*Lee, Lee, & Park, 2018*)**.** *For a symmetric positive definite matrix* R*, the following inequality holds for all differentiable functions* $\{x(t)|t \in [a, b]\}$ *:*

$$-\int_{a}^{b} \dot{x}^T(s)R\dot{x}(s)\,ds \le \Omega^T \left[\sum_{i=1}^{3} \frac{b-a}{2i-1} M_i R^{-1} M_i^T + \sum_{i=1}^{3} Sym\{M_i E_i\} \right] \Omega$$

where

$$E_1\Omega = x(b) - x(a)$$

$$E_2\Omega = x(b) + x(a) - \frac{2}{b-a}\int_a^b x(s)ds$$

$$E_3\Omega = x(b) - x(a) + \frac{6}{b-a}\int_a^b x(s)ds - \frac{12}{(b-a)^2}\int_a^b\int_{\theta}^{b} x(s)ds d\theta.$$

3. Main results

In this section, we investigate into establishing conditions ensuring the exponential stochastic stability of the sliding error motion, as given by (10). We adopt a methodology rooted in the LKF approach and its robustness in analyzing dynamic systems. To initiate our analysis, we introduce relevant definitions and subsequently derive key stability criteria essential for our investigation.

$$\chi(t) = \Big[e^T(t) \quad e^T(t-d(t)) \quad e^T(t-d) \quad h^T(D(e(t))) \quad \int_{t-d(t)}^{t} h^T(D(e(s)))ds$$
$$\frac{1}{d(t)}\int_{t-d(t)}^{t} e^T(s)ds \quad \frac{1}{d-d(t)}\int_{t-d}^{t-d(t)} e^T(s)ds$$
$$\frac{1}{d^2(t)}\int_{t-d(t)}^{t}\int_{s}^{t} e^T(s)ds d\theta$$
$$\frac{1}{(d-d(t))^2}\int_{t-d}^{t-d(t)}\int_{s}^{t-d(t)} e^T(s)ds d\theta \quad \dot{e}^T(t)\Big]^T,$$

$$e_s = \Big[(I_N \otimes (A_i - W_i K_i)) + c_1(G \otimes \Gamma_{1i}) \quad (I_N \otimes B_i) + c_2(G \otimes \Gamma_{2i}) \quad 0$$
$$(I_N \otimes (C_i - W_i \bar{V}_i C_i)) \quad 0_{n\times 5n}\Big],$$

$$e_m = \begin{bmatrix} 0_{n\times(m-1)n} & I_n & 0_{n\times(10-m)n} \end{bmatrix}, \quad m = (1, 2, \dots, 10).$$

Theorem 3.1. *For given scalars* d *and* μ*, and known matrices* K_i *and* $\mathcal{V}i$*, the MJCDNs Lur'e systems* (1) *and* (2) *exhibit exponential synchronization under the sliding surface function provided by* (8)*. At the same time, the dynamic error system* (10) *shows exponential synchronization. This is guaranteed if there exist positive definite matrices* P_i*,* Q_r $(r = 1, 2, 3, 4)$*,* M_l*,* N_l $(l = 1, 2, \dots, 5)$*,* R_a*,* R_b*,* $R_1^{2\times 2}$*, any matrix* $\mathcal{G}$ *of appropriate dimensions, and a positive diagonal matrix* Λ*, such that the following LMIs apply to all* $i \in S$*:*

$$\Xi_1 = \begin{bmatrix} \Sigma_{10\times 10}(d(t) = d) & \Pi_1 \\ * & \bar{\Pi}_1 \end{bmatrix} < 0, \tag{12}$$

$$\Xi_2 = \begin{bmatrix} \Sigma_{10\times 10}(d(t) = 0) & \Pi_2 \\ * & \bar{\Pi}_2 \end{bmatrix} < 0, \tag{13}$$

where $\Sigma = Y_1 + Y_1 + Y_2 + Y_{3a} + Y_4 + Y_{5a} + Y_{5b} + Y_6 + Y_{6a}$*,*

$$Y_1 = 2e_1\Big(I_N \otimes P_i\Big)e_{10}^T + \sum_{j=1}^{S} \phi_{ij} e_1 (I_N \otimes P_j) e_1^T,$$

$$Y_2 = e^{2\alpha d} e_1 Q_1 e_1^T - (1-\mu)e_2 Q_1 e_2^T + e^{2\alpha d} e_1 Q_2 e_1^T - e_3 Q_2 e_3^T$$
$$Y_{3a} = d^2 e^{2\alpha d} e_{10} Q_3 e_{10}^T + sym(M_1\Lambda_1 + M_2\Lambda_2 + M_3\Lambda_3)$$
$$+ sym(N_1\Lambda_4 + N_2\Lambda_5 + N_3\Lambda_6),$$
$$Y_4 = d^2 e^{2\alpha d} e_4 Q_4 e_4^T - e^{-2\alpha d} e_5 Q_4 e_5^T,$$
$$Y_{5a} = d[e_1 \ e_s]R_1[e_1 \ e_s]^T,$$
$$Y_{5b} = e^{\alpha d}[e_1 R_a e_1^T + e_2(R_b - R_a)e_2^T - e_3 R_b e_3^T]$$
$$+ e^{\alpha d} Sym\{M_4\Lambda_7 + M_5\Lambda_8\} + Sym\{N_4\Lambda_9 + N_4\Lambda_{10}\},$$
$$Y_6 = -e_1\Lambda L_1 e_1^T + 2e_1 L_2 e_4^T - e_4\Lambda e_4^T,$$
$$Y_{6a} = 2[e_1 + e_{10}]\mathcal{G}[(I_N \otimes (A_i - W_i K_i))e_1^T$$
$$+ (I_N \otimes B_i)e_2^T + (I_N \otimes (C_i - W_i\bar{V}_i C_i))e_4^T$$
$$+ c_1(G \otimes \Gamma_{1i})e_1^T + c_2(G \otimes \Gamma_{2i})e_2^T],$$

$$\tilde{R}_a = R_1 + \begin{bmatrix} 0 & R_a \\ * & 0 \end{bmatrix}, \ \tilde{R}_b = R_1 + \begin{bmatrix} 0 & R_b \\ * & 0 \end{bmatrix},$$

$$\Lambda_1^T = e_1 - e_2, \ \Lambda_2^T = e_1 + e_2 - 2e_6, \ \Lambda_3^T = e_1 - e_2 + 6e_6 - 12e_8,$$
$$\Lambda_4^T = e_2 - e_3, \ \Lambda_5^T = e_2 + e_3 - 2e_7, \ \Lambda_6^T = e_2 - e_3 + 6e_7 - 12e_9,$$
$$\Lambda_7^T = [d(t)e_6 \ e_1 - e_2], \ \Lambda_8^T = [d(t)(-e_6 + 2e_8) \ e_1 + e_2 - 2e_6],$$
$$\Lambda_9^T = [(d - d(t))e_7 \ e_2 - e_3], \ \Lambda_{10}^T = [(d - d(t))(-e_7 + 2e_9) \ e_2 + e_3 - 2e_7],$$
$$\Pi_1 = [d M_1 \ d M_2 \ d M_3 \ d M_4 \ d M_5], \ \Pi_2 = [d N_1 \ d N_2 \ d N_3 \ d N_4 \ d N_5],$$
$$\bar{\Pi}_1 = diag\{-dQ_3 \ -3dQ_3 \ -5dQ_3 \ -d\tilde{R}_a \ -3d\tilde{R}_a\},$$
$$\bar{\Pi}_2 = diag\{-dQ_3 \ -3dQ_3 \ -5dQ_3 \ -d\tilde{R}_b \ -3d\tilde{R}_b\},$$

Proof. Define Lyapunov–Krasovskii functional as

$$V(e(t), t, i) = \sum_{r=1}^{5} V_r(e(t), t, i), \tag{14}$$

where

$$V_1(e(t), t, i) = e^{2\alpha t} e^T(t) P_i e(t),$$
$$V_2(e(t), t, i) = e^{2\alpha d}\int_{t-d(t)}^{t} e^{2\alpha s} e^T(s) Q_1 e(s) ds + e^{2\alpha d}\int_{t-d}^{t} e^{2\alpha s} e^T(s) Q_2 e(s) ds,$$
$$V_3(e(t), t, i) = e^{2\alpha d}\int_{-d}^{0}\int_{t+\beta}^{t} e^{2\alpha s}\dot{e}^T(s) Q_3 \dot{e}(s) ds d\beta,$$
$$V_4(e(t), t, i) = d e^{2\alpha d}\int_{-d}^{0}\int_{t+\beta}^{t} e^{2\alpha s} h^T(De(s)) Q_4 h(De(s)) ds d\beta,$$
$$V_5(e(t), t, i) = e^{2\alpha d}\int_{-d}^{0}\int_{t+\beta}^{t} e^{2\alpha s}\varepsilon^T(s) R_1 \varepsilon(s) ds d\beta,$$

where, $\varepsilon(t) = [e^T(t) \ \ \dot{e}^T(t)]^T$.

Exploring the definition of the infinitesimal operator $\mathcal{L}$ within the LKF, as outlined in Chen et al. (2013), we have the following equality

$$\mathcal{L}V(e_k(t), t, i) = \lim_{\Delta t\to 0} \frac{\mathbb{E}\{V(e(t+\Delta t), t+\Delta t, r(t+\Delta t))|e(t), t, i\} - V(e_k(t), t, i)}{\Delta t}$$
$$= V(e(t), t, i) + \dot{e}^T(t)V(e(t), t, i) + \sum_{j=1}^{S} \phi_{ij} V(e(t), t, j). \tag{15}$$

We derive the infinitesimal generator of the LKF while tracing the trajectory of the error sliding mode dynamics given by (4)

$$\mathcal{L}V_1(e_k(t), t, i) = e^{2\alpha t}\left[2e^T(t)P_i\dot{e}(t) + \sum_{j=1}^{S}\phi_{ij}e^T(t)(P_j)e(t)\right],$$
$$= e^{2\alpha t}\left[2e^T(t)P_i\dot{e}(t) + \sum_{j=1}^{S}\phi_{ij}e^T(t)(I \otimes P_j)e(t)\right],$$

$$\mathcal{L}V_1(e_k(t), t, i) = e^{2\alpha t}\chi^T(t)Y_1\chi(t), \tag{16}$$

$$\mathcal{L}V_2(e_k(t), t, i) = e^{2\alpha t}e^{2\alpha d}e^T(t)Q_1e(t) - e^{2\alpha t}(1-\mu)e^T(t-d(t))Q_1e(t-d(t))$$
$$+ e^{2\alpha t}e^{2\alpha d}e^T(t)Q_2e(t) - e^{2\alpha t}e^T(t-d)Q_2e(t-d),$$

$$\mathcal{L}V_2(e_k(t), t, i) = e^{2\alpha t}\chi^T(t)Y_2\chi(t), \tag{17}$$

$$\mathcal{L}V_3(e_k(t), t, i) = d^2e^{2\alpha t}e^{2\alpha d}\dot{e}^T(t)Q_3\dot{e}(t) - de^{2\alpha t}\int_{t-d}^{t}\dot{e}^T(s)Q_3\dot{e}(s)ds, \tag{18}$$

$$\mathcal{L}V_4(e_k(t),t,i) = d^2e^{2\alpha t}e^{2\alpha d}h^T(De(t))Q_4h(De(t)) - de^{2\alpha t}\int_{t-d}^{t}h^T(De(s))Q_4h(De(s))ds, \tag{19}$$

$$\mathcal{L}V_5(e_k(t),t,i) = d^2e^{2\alpha t}e^{2\alpha d}\varepsilon^T(t)R_1\varepsilon(t) - de^{2\alpha t}\int_{t-d}^{t}\varepsilon^T(s)R_1\varepsilon(s)ds. \tag{20}$$

Notice (18) of Lemma 2.4, then

$$\begin{aligned}\int_{t-d}^{t}\dot{e}^T(s)Q_3\dot{e}(s)ds &\le -\int_{t-d(t)}^{t}\dot{e}^T(s)Q_3\dot{e}(s)ds - \int_{t-d}^{t-d(t)}\dot{e}^T(s)Q_3\dot{e}(s)ds,\\ &\le \chi^T(t)\Bigg\{d(t)\Big(M_1Q_3^{-1}M_1^T + \frac{1}{3}M_2Q_3^{-1}M_2^T + \frac{1}{5}M_3Q_3^{-1}M_3^T\Big)\\ &+ sym(M_1\Lambda_1 + M_2\Lambda_2 + M_3\Lambda_3) + (d-d(t))\Big(N_1Q_3^{-1}N_1^T\\ &+ \frac{1}{3}N_2Q_3^{-1}N_2^T + \frac{1}{5}N_3Q_3^{-1}N_3^T\Big) + sym(N_1\Lambda_4 + N_2\Lambda_5 + N_3\Lambda_6)\Bigg\}\chi(t),\end{aligned}$$

$$\mathcal{L}V_3(e_k(t),t,i) \le e^{2\alpha t}\chi^T(t)(Y_{3a}+Y_{3b})\chi(t) \tag{21}$$

where $Y_{3b} = d(t)\Big(M_1Q_3^{-1}M_1^T + \frac{1}{3}M_2Q_3^{-1}M_2^T + \frac{1}{5}M_3Q_3^{-1}M_3^T\Big)$.

$$de^{2\alpha t}\int_{t-d}^{t}h^T(De(s))Q_4h(De(s))ds \le e^{-2\alpha d}\int_{t-d}^{t}h^T(De(s))Q_4\int_{t-d}^{t}h(De(s))ds,$$

$$\mathcal{L}V_4(e_k(t),t,i) \le e^{2\alpha t}\chi^T(t)Y_4\chi(t) \tag{22}$$

Further, from the (20) we can calculate as follows,

$$-\int_{t-d}^{t}\varepsilon^T(s)R_1\varepsilon(s)ds = -\int_{t-d(t)}^{t}\varepsilon^T(s)R_1\varepsilon(s)ds - \int_{t-d}^{t-d(t)}\varepsilon^T(s)R_1\varepsilon(s)ds,$$

inspired by Hua, Wang, and Wu (2019) and we can derive the following

$$0 = e^T(t)R_ae(t) - e^T(t-d(t))R_ae(t-d(t)) - 2\int_{t-d(t)}^{t}e^T(s)R_a\dot{e}(s)ds, \tag{23}$$

$$0 = e^T(t-d(t))R_be(t-d(t)) - e^T(t-d)R_be(t-d) - 2\int_{t-d}^{t-d(t)}e^T(s)R_b\dot{e}(s)ds. \tag{24}$$

By using above equation with Lemma 2.3, we can deduce

$$\begin{aligned}\mathcal{L}V_5(e_k(t),t,i) &= d^2e^{2\alpha t}e^{2\alpha d}\chi^T(t)Y_5\chi(t)\\ &- e^{2\alpha t}\int_{t-d(t)}^{t}\varepsilon^T(s)R_1\varepsilon(s)ds - e^{2\alpha t}\int_{t-d}^{t-d(t)}\varepsilon^T(s)R_1\varepsilon(s)ds\\ &- 2\int_{t-d(t)}^{t}e^T(s)R_a\dot{e}(s)ds - 2\int_{t-d}^{t-d(t)}e^T(s)R_b\dot{e}(s)ds,\\ &= d^2e^{2\alpha t}e^{2\alpha d}\chi^T(t)Y_{5a}\chi(t) - e^{2\alpha t}\int_{t-d(t)}^{t}\varepsilon^T(s)\tilde{R}_a\varepsilon(s)ds\\ &- e^{2\alpha t}\int_{t-d}^{t-d(t)}\varepsilon^T(s)\tilde{R}_b\varepsilon(s)ds\end{aligned} \tag{25}$$

For any matrices M_4, M_5, N_4, and N_5 we can get

$$\begin{aligned}&-e^{2\alpha t}\int_{t-d(t)}^{t}\varepsilon^T(s)\tilde{R}_a\varepsilon(s)ds - e^{2\alpha t}\int_{t-h}^{t-d(t)}\varepsilon^T(s)\tilde{R}_b\varepsilon(s)ds\\ &\le e^{2\alpha t}\chi^T(t)\Bigg\{d(t)\Big(M_4\tilde{R}_a^{-1}M_4^T + \frac{1}{3}M_5\tilde{R}_a^{-1}M_5^T\Big) + sym\{M_4\Lambda_7 + M_5\Lambda_8\}\\ &+ (d-d(t))\Big(N_4\tilde{R}_b^{-1}N_4^T + \frac{1}{3}N_5\tilde{R}_b^{-1}N_5^T\Big) + sym\{N_4\Lambda_9 + N_5\Lambda_{10}\}\Bigg\}\chi(t).\end{aligned} \tag{26}$$

$$\mathcal{L}V_5(e_k(t),t,i) = d^2e^{2\alpha t}\chi^T(t)[e^{2\alpha d}Y_{5a} + Y_{5b} + Y_{5c}]\chi(t), \tag{27}$$

where $Y_{5c} = d(t)\Big(M_4\tilde{R}_a^{-1}M_4^T + \frac{1}{3}M_5\tilde{R}_a^{-1}M_5^T\Big) + (d-d(t))\Big(N_4\tilde{R}_b^{-1}N_4^T + \frac{1}{3}N_5\tilde{R}_b^{-1}N_5^T\Big)$.

For any appropriate dimension matrix $\mathcal{G}$, we can consider the following equality,

$$\begin{aligned}0 = 2[e(t)+\dot{e}(t)]^T\mathcal{G}[(I_N\otimes(A_i - W_iK_i))e(t)(I_N\otimes B_i)e(t-d(t))\\ + (I_N\otimes(C_i - W_i\bar{V}_iC_i))h(De(t)) + c_1(G\otimes\Gamma_{1i})e(t) + c_2(G\otimes\Gamma_{2i}e(t-d(t)))].\end{aligned} \tag{28}$$

On the other hand, for any diagonal matrix Λ, it can be found that,

$$e^{2\alpha t}\begin{pmatrix} e(t)\\ h(De(t))\end{pmatrix}^T\begin{pmatrix} D^TL_1\Lambda D & -D^TL_2\Lambda\\ * & \Lambda\end{pmatrix}\begin{pmatrix} e(t)\\ h(De(t))\end{pmatrix} \ge 0,$$

$$e^{2\alpha t}\Big[-e^T(t)D^T\Lambda L_1De(t) + 2e^T(t)D^TL_2h(D(e(t))) - h^T(D(e(t)))\Lambda h(D(e(t)))\Big] \le 0,$$

$$e^{2\alpha t}\chi^T(t)Y_6\chi(t) \le 0. \tag{29}$$

Then, from (16)–(29) it can be yields

$$\mathcal{L}V(e_k(t),t,i) \le e^{2\alpha t}\chi^T(t)[\Sigma + Y_{3b} + Y_{5c}]\chi(t), \tag{30}$$

by using the Schur complement in (30), one can get $\Xi_i < 0$, where Ξ_i $(i = 1,2)$ is defined in (12) and (13), which implies that,

$$\mathcal{L}V(e_k(t),t,i) \le 0.$$

Following the similar line in He, Wu, and She (2006), we have

$$\lambda_{\min}(P_i)e^{-2\alpha t}\mathbb{E}\{\|e(t)\|^2\} \le \mathbb{E}\{V(e_k(t),t,i)\} \le \mathbb{E}\{V(e(0))\},$$

From the (14), we can get the following,

$$\mathbb{E}\{V(e(0))\} \le \mathbb{E}\nabla\sup_{-d\le t\le 0}\{\|e(t)\|^2, \|\dot{e}(t)\|^2\} \tag{31}$$

where

$$\nabla = \lambda_{\max}(Q_1) + \lambda_{\max}(Q_2) + d\lambda_{\max}(Q_3) + d^2\lambda_{\max}(Q_4) + d\lambda_{\max}(R_1)$$

It is come to know that

$$\mathbb{E}V(e(t)) \le \mathbb{E}V(0)e^{-2\alpha t} \le \mathbb{E}\nabla e^{-2\alpha t}\sup_{-d\le t\le 0}\{\|e(t)\|^2, \|\dot{e}(t)\|^2\} \tag{32}$$

Thus, one has

$$\mathbb{E}\|e(t)\|^2 \le \frac{\nabla}{\lambda_{min}(P)}e^{-\alpha t}\sup_{-d\le t\le 0}\{\|e(t)\|^2, \|\dot{e}(t)\|^2\}. \tag{33}$$

By Definition 2.1, the error sliding mode dynamics (10) can be exponentially stable, which means the CDNs (1) is exponentially synchronized with (2). This completes the proof.

Theorem 3.2. *Given scalars d and μ, and the known matrix $\mathcal{V}_i$, the MJCDNs Lur'e system (1) and (2) are exponential synchronize under the sliding surface function given by (8), the error dynamic system (10) is exponentially stable. If there exist positive definite matrices $\overline{P}_i$, $\overline{Q}_r$ $(r = 1,2,3,4)$, $\overline{M}_l$, $\overline{N}_l$ $(l = 1,2,\dots,5)$, $\overline{R}_a$, $\overline{R}_b$, $\overline{R}_1^{2\times 2}$, any matrix $Y_i > 0$ and $\mathfrak{M}$ of appropriate dimensions and positive diagonal matrix Λ such that the following LMIs hold for all $i \in S$:*

$$\overline{\Xi}_1 = \begin{bmatrix}\overline{\Sigma}_{10\times 10}(d(t)=d) & \overline{\Pi}_1\\ * & \hat{\Pi}_1\end{bmatrix} < 0, \tag{34}$$

$$\overline{\Xi}_2 = \begin{bmatrix}\overline{\Sigma}_{10\times 10}(d(t)=0) & \overline{\Pi}_2\\ * & \hat{\Pi}_2\end{bmatrix} < 0, \tag{35}$$

where $\overline{\Sigma} = \overline{Y}_1 + \overline{Y}_1 + \overline{Y}_2 + \overline{Y}_{3a} + \overline{Y}_4 + \overline{Y}_{5a} + \overline{Y}_{5b} + \overline{Y}_6 + \overline{Y}_{6a}$

$$\begin{aligned}\overline{Y}_1 &= 2e_1\Big(I_N\otimes\overline{P}_i\Big)e_{10}^T + \sum_{j=1}^{S}\phi_{ij}e_1(I\otimes\overline{P}_j)e_1^T,\\ \overline{Y}_2 &= e^{2\alpha d}e_1\overline{Q}_1e_1^T - (1-\mu)e_2\overline{Q}_1e_2^T + e^{2\alpha d}e_1\overline{Q}_2e_1^T - e_3\overline{Q}_2e_3^T\\ \overline{Y}_{3a} &= d^2e^{2\alpha d}e_{10}\overline{Q}_3e_{10}^T + sym(\overline{M}_1\Lambda_1 + \overline{M}_2\Lambda_2 + \overline{M}_3\Lambda_3)\\ &\quad + sym(\overline{N}_1\Lambda_4 + \overline{N}_2\Lambda_5 + \overline{N}_3\Lambda_6),\\ \overline{Y}_4 &= d^2e^{2\alpha d}e_4\overline{Q}_4e_4^T - e^{-2\alpha d}e_5\overline{Q}_4e_5^T,\\ \overline{Y}_{5a} &= d[e_1\ e_s]\overline{R}_1[e_1\ e_s]^T,\\ \overline{Y}_{5b} &= e^{\alpha d}[e_1\overline{R}_ae_1^T + e_2(\overline{R}_b - \overline{R}_a)e_2^T - e_3\overline{R}_be_3^T]\\ &\quad + e^{\alpha d}Sym\{\overline{M}_4\Lambda_7 + \overline{M}_5\Lambda_8\} + Sym\{\overline{N}_4\Lambda_9 + \overline{N}_4\Lambda_{10}\},\end{aligned}$$

$$\overline{Y}_6 = -e_1\overline{\Lambda}L_1e_1^T + 2e_1L_2e_4^T - e_4\overline{\Lambda}e_4^T,$$
$$\begin{aligned}\overline{Y}_{6a} &= 2e_1[(I_N\otimes(A_i)\mathfrak{M} - W_iY_i)e_1^T + (I_N\otimes B_i)\mathfrak{M}e_2^T\\ &+ (I_N\otimes(C_i - W_i\bar{V}_iC_i)\mathfrak{M})e_4^T\\ &+ c_1(G\otimes\Gamma_{1i})\mathfrak{M}e_1^T + c_2(G\otimes\Gamma_{2i})\mathfrak{M}e_2^T]\\ &+ 2e_{10}[(I_N\otimes(A_i)\mathfrak{M} - W_iY_i)e_1^T + (I_N\otimes B_i)\mathfrak{M}e_2^T\\ &+ (I_N\otimes(C_i - W_i\bar{V}_iC_i)\mathfrak{M})e_4^T + c_1(G\otimes\Gamma_{1i})\mathfrak{M}e_1^T + c_2(G\otimes\Gamma_{2i})\mathfrak{M}e_2^T],\end{aligned}$$
$$\hat{R}_a = \overline{R}_1 + \begin{bmatrix}0 & \overline{R}_a\\ * & 0\end{bmatrix},\ \hat{R}_b = \overline{R}_1 + \begin{bmatrix}0 & \overline{R}_b\\ * & 0\end{bmatrix},$$
$$\Lambda_1^T = e_1 - e_2,\ \Lambda_2^T = e_1 + e_2 - 2e_5,\ \Lambda_3^T = e_1 - e_2 + 6e_6 - 12e_8,$$
$$\Lambda_4^T = e_2 - e_3,\ \Lambda_5^T = e_2 + e_3 - 2e_7,\ \Lambda_6^T = e_2 - e_3 + 6e_7 - 12e_9,$$
$$\Lambda_7^T = [d(t)e_6\ e_1 - e_2],\ \Lambda_8^T = [d(t)(-e_6 + 2e_8)\ e_1 + e_2 - 2e_6],$$
$$\Lambda_9^T = [(d - d(t))e_7\ e_2 - e_3],\ \Lambda_{10}^T = [(d - d(t))(-e_7 + 2e_9)\ e_2 + e_3 - 2e_7],$$
$$\Pi_1 = [d\overline{M}_1\ d\overline{M}_2\ d\overline{M}_3\ d\overline{M}_4\ d\overline{M}_5],\ \Pi_2 = [d\overline{N}_1\ d\overline{N}_2\ d\overline{N}_3\ d\overline{N}_4\ d\overline{N}_5],$$
$$\bar{\Pi}_1 = diag\{-d\overline{Q}_3\ -3d\overline{Q}_3\ -5d\overline{Q}_3\ -d\hat{R}_a\ -3d\hat{R}_a\},$$
$$\bar{\Pi}_2 = diag\{-d\overline{Q}_3\ -3d\overline{Q}_3\ -5d\overline{Q}_3\ -d\hat{R}_b\ -3d\hat{R}_b\}.$$

Then the sliding mode control law is given by $K_i = Y_i\mathfrak{M}^{-1}$.

Proof. Denote the following new matrix variables $\mathcal{G}^{-1} = \mathfrak{M}$, $\overline{P}_i = \mathfrak{M}P_i\mathfrak{M}^T$, $\overline{Q}_r = \mathfrak{M}Q_r\mathfrak{M}^T$ $(r = 1,2,3,4)$, $\overline{M}_r = \mathfrak{M}M_r\mathfrak{M}^T$ $(r = 1,\dots,5)$, $\overline{N}_r = \mathfrak{M}N_r\mathfrak{M}^T$ $(r = 1,\dots,5)$, $\overline{R}_1 = \mathfrak{M}R_1\mathfrak{M}^T$, $\overline{R}_a = \mathfrak{M}R_a\mathfrak{M}^T$, $\overline{R}_b = \mathfrak{M}R_b\mathfrak{M}^T$, pre- and post-multiplying (12) and (13) by diag $\{\mathfrak{M}\ \mathfrak{M}\ \mathfrak{M}\ \mathfrak{M}\ \mathfrak{M}\ \mathfrak{M}\ \mathfrak{M}\ \mathfrak{M}\ \mathfrak{M}\ \mathfrak{M}\mathfrak{M}\ \mathfrak{M}\ \mathfrak{M}\ \mathfrak{M}\ \mathfrak{M}\}$ and its transpose and applying Schur complement, it is straightforward to get the LMIs (34) and (35).

Remark 3.3. We can further investigate the effectiveness of our exponential synchronization criteria by examining a special case of complex dynamical networks described by (1) and (2). Specifically, we will consider a simplified scenario where the system can be described by complex dynamical networks without the Markovian jump ($r_t = 0$). In this case, the error system (10) is modeled as an equation of the form

$$\begin{aligned}\dot{e}(t) =&(I_N\otimes(A - WK))e(t)(I_N\otimes B)e(t - d(t))\\ &+ (I_N\otimes(C - W\bar{V}C))h(De(t))\\ &+ c_1(G\otimes\Gamma_1)e(t) + c_2(G\otimes\Gamma_2e(t - d(t))),\end{aligned} \tag{36}$$

By analyzing this simplified case, we employ the same proof line in Theorem 3.1, and we can achieve the system (36) is exponentially stable.

B. Reachability analysis

The following Theorem 3.4 presents a methodology for designing a control law that facilitates the global convergence of system state trajectories to a predefined switching surface within a finite duration. Subsequently, the control law ensures the sustained maintenance of trajectories on this surface, regardless of initial conditions, thereby fostering stable system behavior.

Theorem 3.4. *Assuming the sliding surface is defined by Eq. (5) and satisfying the LMI condition as outlined in Theorem 3.1, the state trajectories of MJCDNs described by Eqs. (1) and (2) can be directed onto the sliding surface* $s_k(t,i) = 0$ *within a finite time by employing the sliding mode control law:*

$$u_k(t) = K_ie_k(t) + \delta_{ki} + \|W_i^{-1}\|(\|C_ih(De_k(t))\|)sign(W_i^T\mathcal{V}_is_k(t,i)), \tag{37}$$

where, for all $i \in S = \{1,2,3,\dots.,m\}$, δ_{ki} *represents a given positive scalar. This control law incorporates terms such as* $K_ie_k(t)$ *and* δ_{ki}, *alongside a term involving* W_i^{-1}, C_i, $h(De_k(t))$, *and* $W_i^T\mathcal{V}_is_k(t,i)$, *ensuring the trajectories' convergence onto and maintenance on the sliding surface.*

Proof. Construct Lyapunov functional as

$$\mathcal{W}(s_k(t,i)) = \frac{1}{2}s_k^T(t,i)s_k(t,i). \tag{38}$$

By examining the time derivative of the sliding mode surface, $s_k(t,i)$, and (5), we obtain

$$\begin{aligned}\dot{\mathcal{W}}(s_k(t,i)) &= s_k^T(t,i)\dot{s}_k(t,i)\\ &= s_k^T(t,i)\mathcal{V}_i\Big\{\dot{e}_k(t) - \Big[(A_i - W_iK_i)e_k(t)\\ &+ c_1\sum_{l=1}^{N}g_{kl}\Gamma_{1i}e_l(t) + B_ie_k(t - d(t))\\ &+ c_2\sum_{l=1}^{N}g_{kl}\Gamma_{2i}e_l(t - d(t))\Big]\Big\}\\ &= s_k^T(t,i)\mathcal{V}_i\Big[W_iK_ie_k(t) + C_ih(De_k(t)) + W_iu_k(t)\Big],\end{aligned} \tag{39}$$
$$\begin{aligned}&= s_k^T(t,i)\mathcal{V}_iW_i\Big[u_k(t) + K_ie_k(t) + W_i^{-1}C_ih(De_k(t))\Big]\\ &\le s_k^T(t,i)V_iW_i\Big[u_k(t) + K_ie_k(t)\Big]\\ &+ \|W_i^{-1}\|\,\|C_ih(De_k(t))\|\cdot\|W_i^T\mathcal{V}_i^Ts_k(t,i)\|\end{aligned} \tag{40}$$

Substituting (37) into (40), which implies that

$$\dot{\mathcal{W}}(s_k(t,i)) \le -\delta_{ki}\|W_i^T\mathcal{V}_i^Ts_k(t,i)\| \le -\sqrt{2}\delta_{ki}\lambda_{min}(\mathcal{V}_iW_i)\mathcal{V}^{\frac{1}{2}}(s_k(t,i))$$

By initializing the sliding mode surface at $t_0 = 0$ with r_0, denoted as s_{k0}, we can derive that

$$\mathbb{E}\{\mathcal{W}(s_k(t,i)) \mid s_{k0}, r_0\}^{\frac{1}{2}} \le -\frac{\sqrt{2}}{2}\delta_{ki}\lambda_{min}(\mathcal{V}_iW_i)t + \mathcal{V}^{\frac{1}{2}}(s_{k0}, r_0) \tag{41}$$

Considering the non-negativity of the left-hand side of Eq. (41), it can be inferred that $\mathcal{W}(s_k(t,i))$ converges to zero within a finite time for each mode $i \in S = 1,2,\dots,m$. This finite time, denoted as t^*, is estimated by:

$$t^* \le \frac{\sqrt{2\mathcal{V}(s_{k0}, r_0)}}{\delta_{ki}\lambda_{min}(\mathcal{V}_iB_i)}$$

Thus, the trajectories of the state for the complex dynamical lure systems described by Eqs. (1) and (2) can be brought onto the sliding surface $s_k(t,i) = 0$ within a finite time. It is imperative that the sliding mode surface $s_k(t,i)$ remains accessible.

Remark 3.5. It is noteworthy that in many industrial processes, the dynamical behaviors are generally complex and non-linear and their genuine mathematical models are always difficult to obtain. How to model the exponential synchronization for Markovian jump Lur'e complex networks with respect to SMC has become one if the main theme in our research work. More particularly, some pioneering works have been done in CDNs with some stability conditions. In Zhong and Song (2023), the problem of synchronization of CDNs have been studied with non-fragile control and fuzzy Markovian modes. Recently, event-triggered and sampled data control was proposed in Rakkiyappan, Latha, and Sivaranjani (2017), Sivaranjani et al. (2018) for CDNs with synchronization approach and Morkov modes. Exponential synchronization of CDNs with hybrid delays has been discussed in Shanmugam, Rhaima, and Ghoudi (2023). The model considered in the present study is more practical than that proposed by Rakkiyappan, Latha, and Sivaranjani (2017), Shanmugam, Rhaima, and Ghoudi (2023), Sivaranjani et al. (2018), Zhong and Song (2023), because they consider usual relevant control has been studied with CDNs based on stabilization conditions, but in this work, we consider a new SMC with the combination of synchronization approach and Markovian jumping modes. Due to the many real-life applications the combined study of CDNs and SMC to the system model is more important. The purpose of this study is to establish Synchronization of these Lure complex networks is achieved through SMC by applying the Lyapunov functional theory and to apply a practical application of the Chua circuit with time series model. Additionally, it is mentioned that, we utilize free weight matrix inequality techniques to estimate the derivative of a Lyapunov functional, such as defined in $\mathcal{L}V_3(e_k(t),t,i), \mathcal{L}V_5(e_k(t),t,i)$,

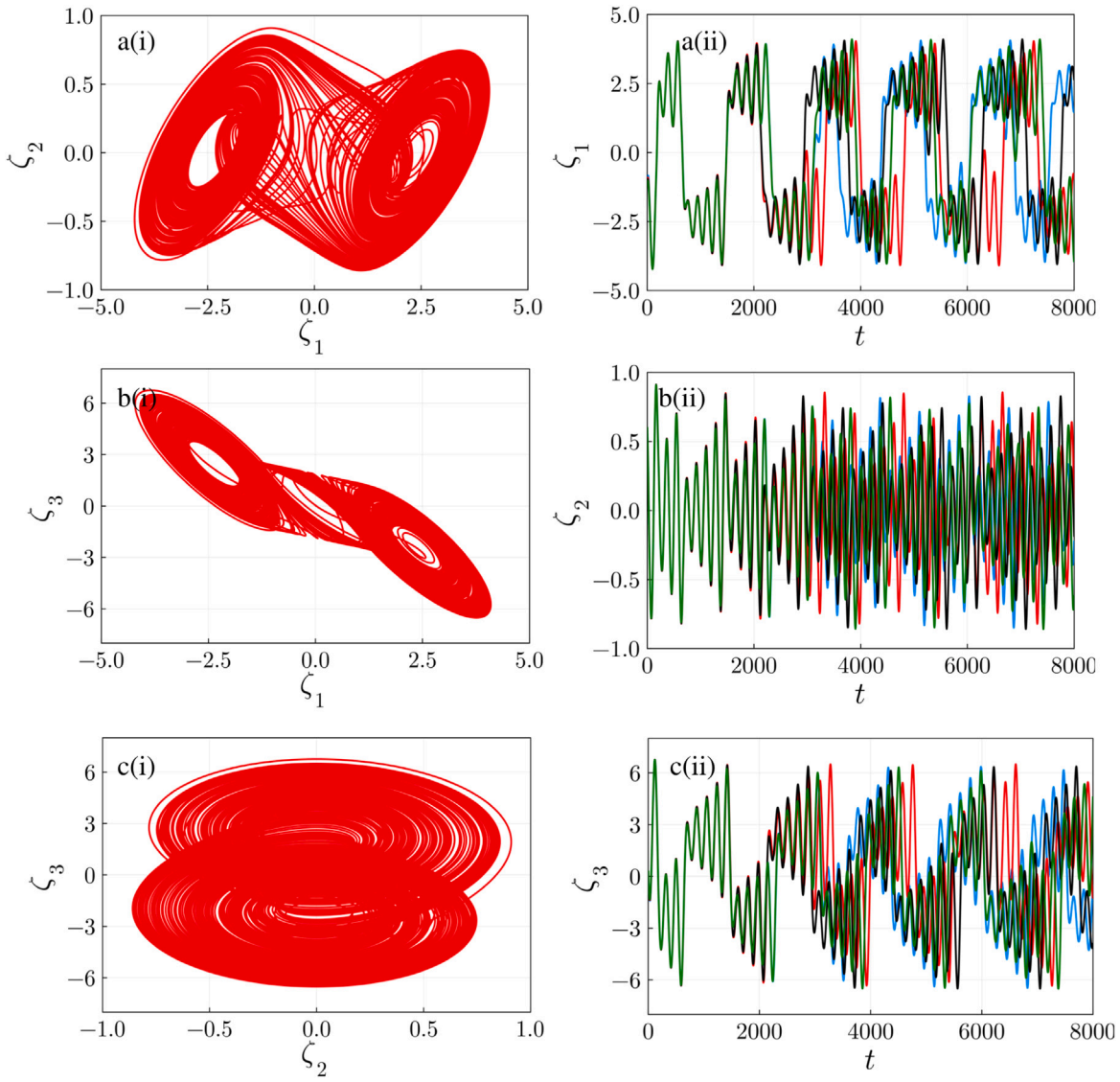

Fig. 1. (a–c) Chaotic behavior of Chua's circuit: (i) Phase portrait and (ii) Time series evaluation for four different initial conditions and other parameters are $m_0 = -0.7$, $m_1 = -1.3$, $a_1 = 10$, $b_1 = 18$ and $\hat{a}_1 = 0.1$ for (42).

which can induce tighter information on the delay of the considered system. Henceforth the investigation procedure and framework model proposed in this paper merit a lot of regard for fill such a demand all the more successfully.

4. Numerical examples

This section introduces two examples utilizing Chua's circuit to illustrate the practical implications and significance of the derived outcomes. Specifically, when employing the theoretical findings with a large node count, solving these LMIs becomes considerably intricate and time-consuming. Consequently, the examples provided below exclusively consider scenarios with a small number of nodes.

Example 4.1. A delayed Chua's circuit configuration can be represented by a two-mode system indexed by $i = 1, 2$. Each node in this system corresponds to a Chua's circuit, as described in Rakkiyappan, Latha, and Sivaranjani (2017). The following description describes how this system operates independently as an isolated node within the larger dynamical network.

$$\dot{\zeta}_1(t) = a_i(\zeta_2(t) - m_1\zeta_1(t) - f(\zeta_1(t))) - \hat{a}_i\zeta_1(t - d(t)),$$
$$\dot{\zeta}_2(t) = \zeta_1(t) - \zeta_2(t) + \zeta_3(t) - \hat{a}_i\zeta_1(t - d(t)),$$
$$\dot{\zeta}_3(t) = -b_i(\zeta_2(t)) + \hat{a}_i(2\zeta_1(t - d(t))) - \zeta_3(t - d(t)), \tag{42}$$

with the nonlinear function

$$f(\zeta_1(t)) = \frac{1}{2}(m_i - m_0)(|\zeta_1(t) + 1| - |\zeta_1(t) - 1|)$$

and the parameters $m_0 = -0.7$, $m_1 = m_2 = -1.3$, $a_1 = 10$, $a_2 = 9.5$, $b_1 = 18$, $b_2 = 17$, $\hat{a}_1 = 0.1$, $\hat{a}_2 = 0.09$, and the time-varying delay $d(t) = |0.5sin(t)|$. Then, system (42) can be represented as a Lur'e dynamical network (10) with four identical nodes (N = 4) with the following parameters

$$A_i = \begin{bmatrix} -a_i m_i & a_i & 0 \\ 1 & -1 & 1 \\ 0 & -a_i & 0 \end{bmatrix}, \; B_i = \begin{bmatrix} -\hat{a}_i & 0 & 0 \\ -\hat{a}_i & 0 & 0 \\ 2\hat{a}_i & 0 & -b \end{bmatrix},$$
$$C_i = \begin{bmatrix} -a_i(m_i - m_0) \\ 0 \\ 0 \end{bmatrix},$$

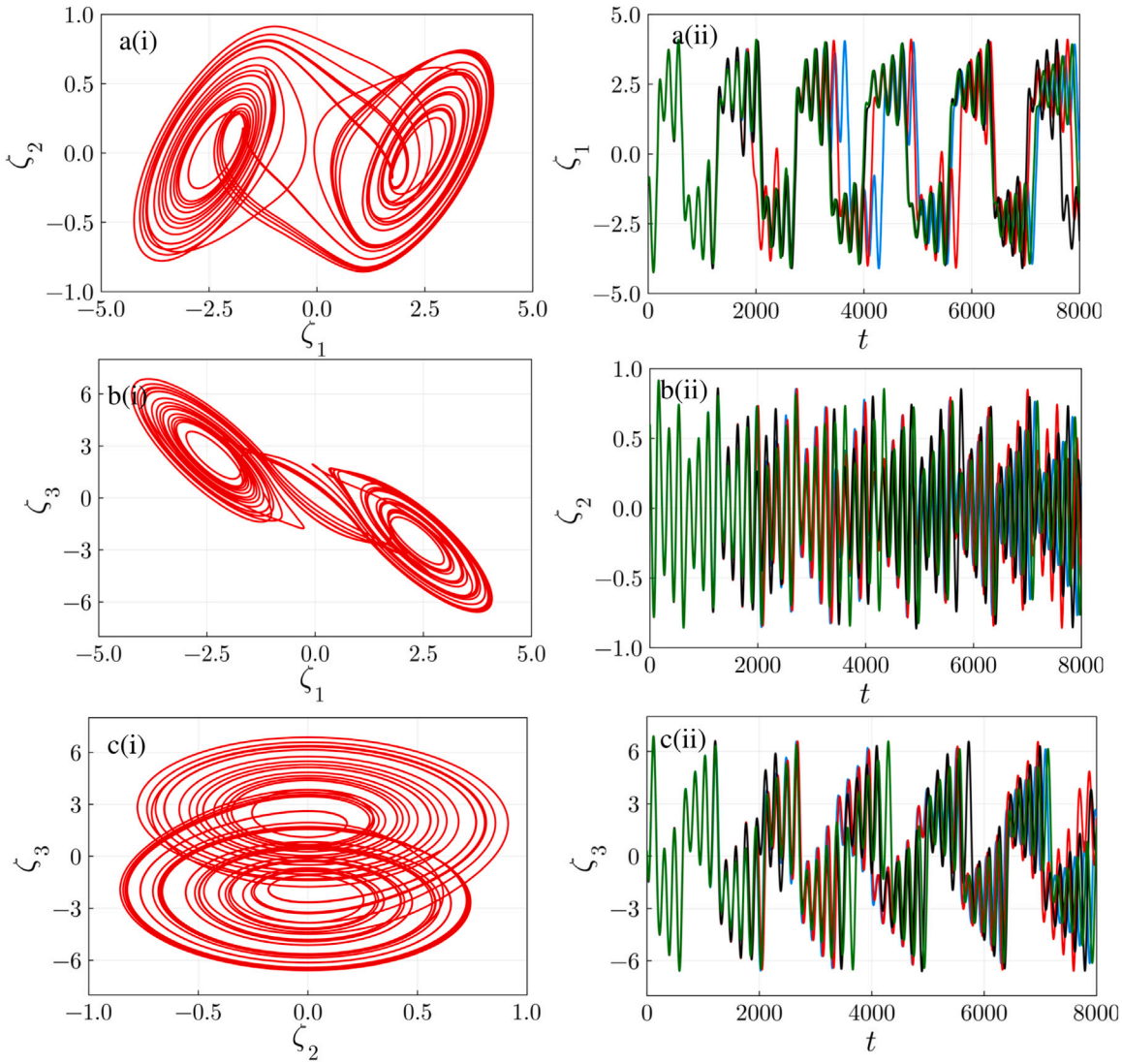

Fig. 2. (a–c) Chaotic behavior of Chua's circuit: (i) Phase portrait and (ii) Time series evaluation for four different initial conditions and system parameters are $m_0 = -0.7$, $m_2 = -1.3$, $a_2 = 9.5$, $b_2 = 17$ and $\hat{a}_2 = 0.09$ for Eq. (42).

$$D_i = \begin{bmatrix} 1 & 0 & 0 \end{bmatrix},\ H = \begin{bmatrix} 1 \\ 2 \\ -1 \end{bmatrix}, G_1 = G_2 = \begin{bmatrix} -2 & 1 & 0 & 1 \\ 1 & -4 & 2 & 1 \\ 0 & 1 & -2 & 1 \\ 0 & 1 & 1 & -2 \end{bmatrix},$$

$$\phi = \begin{bmatrix} -1.2 & 0.8 & 0.4 \\ 1.1 & -2.3 & 1.2 \\ 0.5 & 0.6 & -1.1 \end{bmatrix},\quad \Gamma_{1i} = \Gamma_{2i} = \begin{bmatrix} 1 & 0 & 0 \\ 0 & 1 & 0 \\ 0 & 0 & 1 \end{bmatrix},$$

$c_1 = 1.0, c_2 = 0.2$

$h(e(t)) = \frac{1}{2}(|e(t)+1| - |e(t)-1|)$ and choosing $v_1^+ = v_2^+ = v_3^+ = 1$, $v_1^- = v_2^- = v_3^- = 0$ and by solving the LMIs given in (34)–(35), we determine the maximum allowable upper bound d for various values of μ, as presented in Table 1. This table illustrates the dependency of the upper bound d on the chosen μ. Subsequently, the computation of controller gain matrices is performed as follows:

$$K_1 = \begin{bmatrix} -0.4368 & 0.2247 & 0.0054 \\ 1.6708 & -0.8340 & -3.4247 \\ -2.9831 & 1.2247 & 6.3616 \end{bmatrix},$$

$$K_2 = \begin{bmatrix} -0.2628 & 0.1820 & -0.6469 \\ 0.2934 & -0.2702 & -0.4910 \\ -0.5169 & 0.1728 & 1.2413 \end{bmatrix}.$$

Based on the above gain matrix we observed the chaotic behaviors shown in Figs. 1 and 2. In Fig. 1(a-c)(i) and Fig. 2(a-c)(i) double scroll chaotic behaviors the plotted different projections of the phase portrait. In order to get a better understanding of chaotic behaviors (sensitive depends on the initial conditions), we used different initial conditions for time series evaluation shown in Fig. 1(a-c)(ii) and Fig. 2(a-c)(ii) respectively, initial conditions are chosen as $(-2.05, 0.1, 0.2)$ (Blue line), $(-2.1, 0.1, 0.2)$ (Red line), $(-2.15, 0.1, 0.2)$ (Black line) and $(-2.2, 0.1, 0.2)$ (Green line). Under sliding mode control the synchronization errors of network (3) are given Fig. 3 with the following initial conditions $e_{i1} = (-0.3, 0.3, -0.5, 0.5)$, $e_{i2} = (-0.3, 0.3, -0.5, 0.5)$ and $e_{i3} = (-0.3, 0.3, -0.5, 0.5)$. The Markovian jump mode and the corresponding state trajectories of the error system (3) with the first variable are displayed in Fig. 3(a). Furthermore, Fig. 3(b) displays the state trajectories of the error system (3) with the second variable and Fig. 3(c) shows the state trajectories of the error system (3) with the third variable. The closed-loop system with the various state responses is simulated in Figs. 4–6. Assume that the random initial values of the master system and the slave system in Figs. 4–6 are initially the responses of the states $x_{k1}(t) - \bar{x}_1(t)$, $x_{k2}(t) - \bar{x}_2(t)$ and $x_{k3}(t) - \bar{x}_3(t)$, where $(k = 1, 2, 3, 4)$. It can be clearly seen that the master and slave models are synchronized with the proposed control scheme. Moreover,

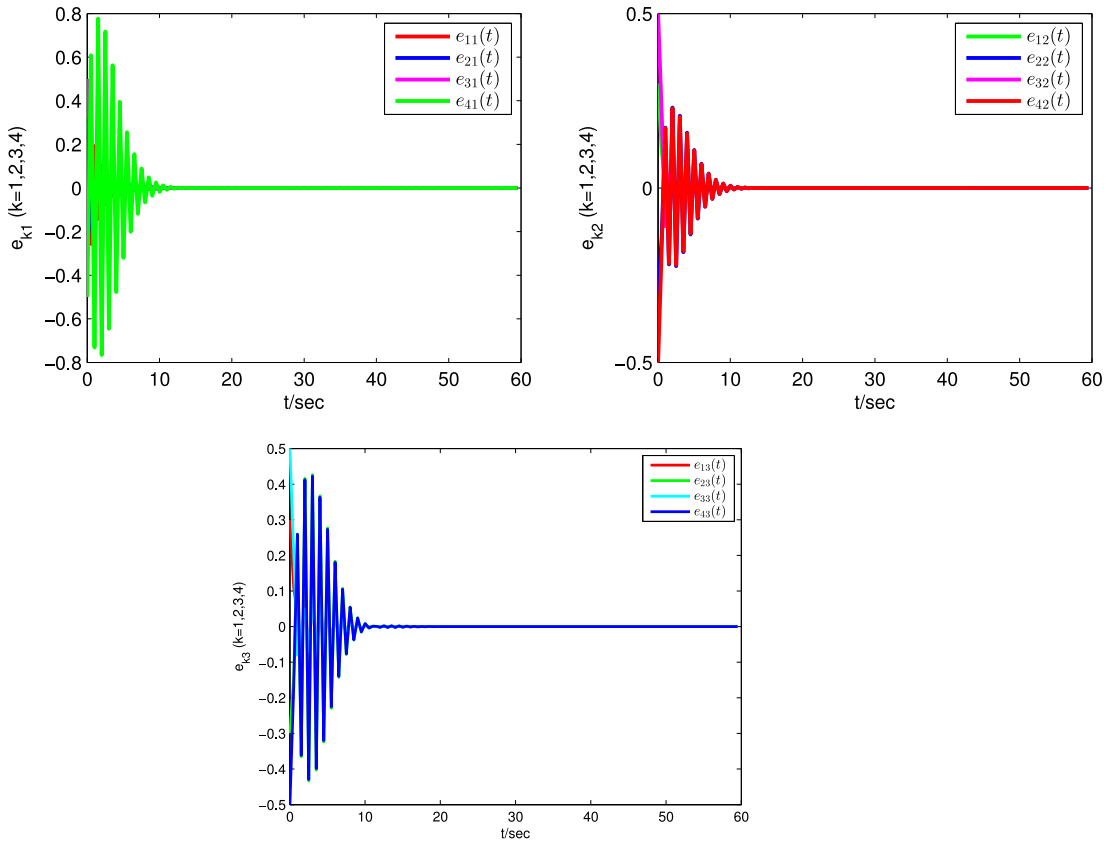

Fig. 3. The state trajectories of errors in Example 4.1.

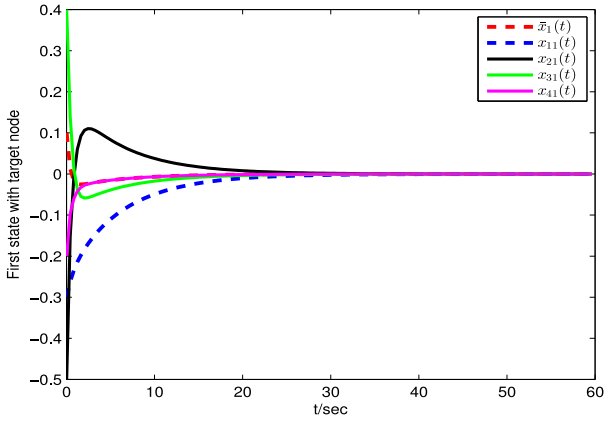

Fig. 4. State Response of $x_{k1}(t)$, $(k = 1, 2, 3, 4)$ and $\bar{x}_1(t)$.

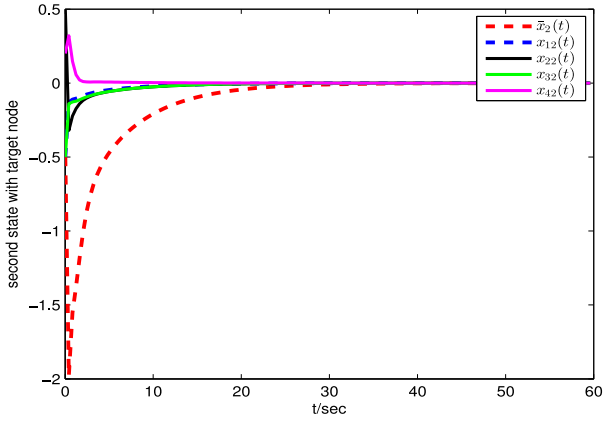

Fig. 5. State Response of $x_{k2}(t)$ $(k = 1, 2, 3, 4)$ and $\bar{x}_2(t)$.

Fig. 7 describes the trajectory of the sliding surface and shows that the sliding surface is continuous. Therefore, the systems (1) and (2) can successfully achieve exponential synchronization.

Example 4.2. Considering the complex dynamical Lure system which is expressed by (10) with 5 nodes and 2 modes, where the known matrices and other parameters are supposed as

Mode: 1

$$A_1 = \begin{bmatrix} -3 & 1 & 0 \\ 1 & -1 & 0.1 \\ 0.3 & 1 & 1 \end{bmatrix}, \quad W_1 = \begin{bmatrix} 1 & 0.2 & 0.5 \\ -0.1 & 2 & 2 \\ 0.2 & 0 & 1.8 \end{bmatrix},$$

$$B_1 = \begin{bmatrix} -0.1 & 0 & 0.2 \\ 0.1 & -1.5 & 0 \\ 0.1 & 0 & -1.3 \end{bmatrix},$$

$$C_1 = \begin{bmatrix} 0.6 & 0 & 1 \\ 1 & 0.2 & 1 \\ 1 & 0.3 & 0.5 \end{bmatrix}, \quad \Gamma_{11} = \begin{bmatrix} 1 & 0 & 0 \\ 0 & 1 & 0 \\ 0 & 0 & 1 \end{bmatrix}, \quad \Gamma_{21} = \begin{bmatrix} 2 & 0 & 0 \\ 0 & 2 & 0 \\ 0 & 0 & 2 \end{bmatrix}$$

Mode: 2

$$A_2 = \begin{bmatrix} -2 & 0.5 & 0 \\ 1 & -2 & 0.1 \\ 0.3 & 0.1 & 1 \end{bmatrix}, \quad W_2 = \begin{bmatrix} 1.2 & 0.3 & 0.2 \\ -0.3 & 1.2 & 0.7 \\ 0.1 & 1.6 & 1.2 \end{bmatrix},$$

$$B_2 = \begin{bmatrix} -0.2 & 0 & 1 \\ -0.2 & 2 & 0 \\ 0.1 & 0 & -3 \end{bmatrix},$$

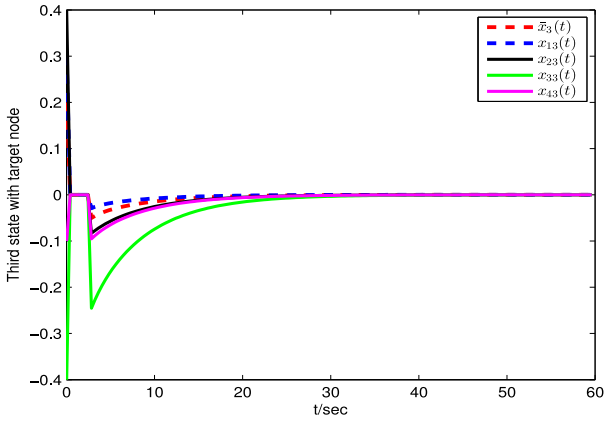

Fig. 6. State Response of $x_{k3}(t)$ $(k = 1, 2, 3, 4)$ and $\bar{x}_3(t)$.

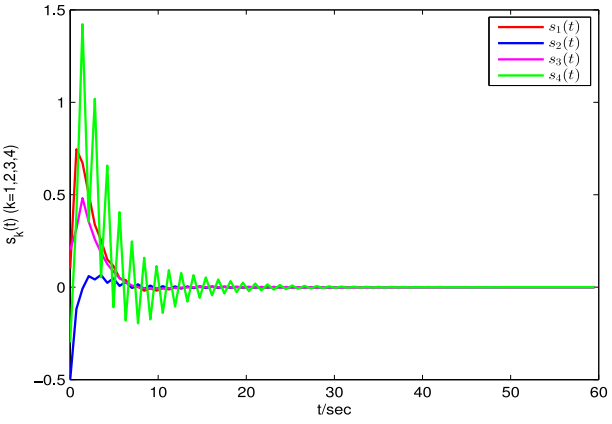

Fig. 7. Sliding mode surface function $s_k(t)$.

$$C_2 = \begin{bmatrix} 0.3 & 0 & 1.3 \\ 1.5 & 0.24 & 1.2 \\ 1.4 & 0.4 & 0.3 \end{bmatrix}, \quad \Gamma_{12} = \begin{bmatrix} 1.5 & 0 & 0 \\ 0 & 1.5 & 0 \\ 0 & 0 & 1.5 \end{bmatrix},$$

$$\Gamma_{22} = \begin{bmatrix} 2.5 & 0 & 0 \\ 0 & 2.5 & 0 \\ 0 & 0 & 2.5 \end{bmatrix},$$

$$G_1 = G_2 = \begin{bmatrix} -3 & 1 & 0 & 2 & 0 \\ 0 & -6 & 0 & 1 & 0 \\ 0.1 & 1 & -2 & 0.3 & 0 \\ 1 & 1 & 0.1 & -0.4 & 0.1 \\ 0 & 0.2 & 0.3 & 1 & -6 \end{bmatrix},$$

$D = diag\{1, 1, 1\}, h(e(t)) = 0.5(|e(t) + 1| - |e(t) - 1|)$. The time-varying delay $d = 1.6$, $\mu = 0.6$. Let us consider the coupling strength $c_1 = c_2 = 1$. The transition rate matrix is $\begin{bmatrix} 0.2 & 0.1 & -0.3 \\ 0.5 & -0.7 & 0.2 \\ -0.6 & 0.1 & 0.5 \end{bmatrix}$, Let us take the matrices L_1 and L_2 as follows: $\begin{bmatrix} 0.5 & 0 & 0 \\ 0 & 0.5 & 0 \\ 0 & 0 & 0.5 \end{bmatrix}$, $\begin{bmatrix} 0.7 & 0 & 0 \\ 0 & 0.7 & 0 \\ 0 & 0 & 0.7 \end{bmatrix}$. The LMIs (34) and (35) in Theorem 3.2 are solved by the MATLAB LMI toolbox, and obtained the solutions of gain matrices K_i are

$$K_1 = \begin{bmatrix} -0.0982 & -0.1983 & -0.2573 \\ -0.1886 & 0.6345 & -0.9231 \\ -0.0335 & -0.6370 & 1.3611 \end{bmatrix},$$

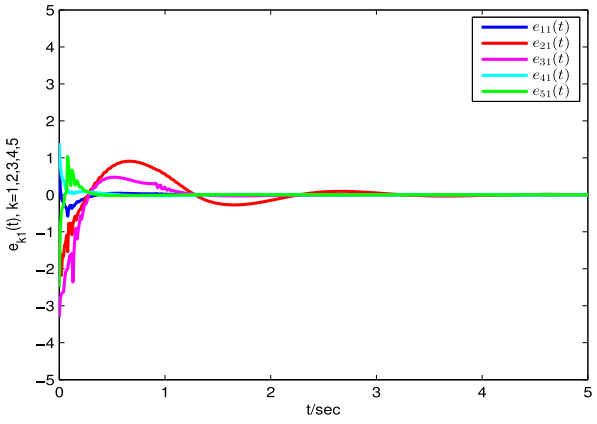

Fig. 8. Trajectories of error system (10) under control schemes.

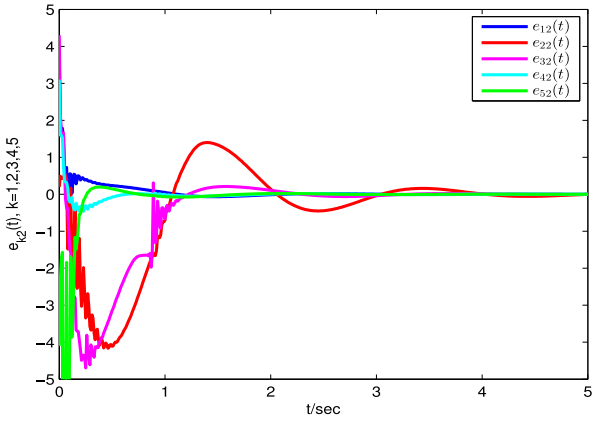

Fig. 9. Trajectories of error system (10) under control schemes.

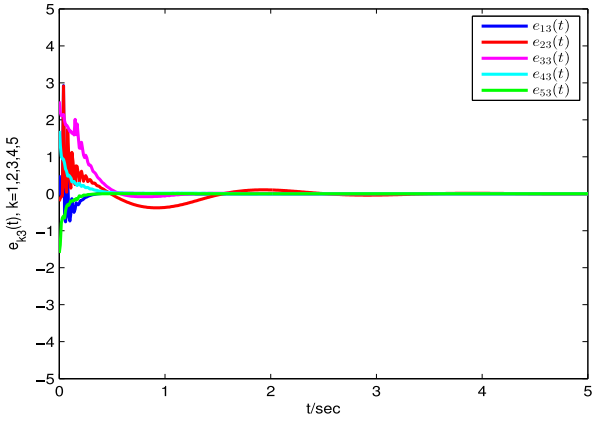

Fig. 10. Trajectories of error system (10) under control schemes.

$$K_2 = \begin{bmatrix} -0.0894 & -0.4392 & 0.3709 \\ -0.1888 & 2.4568 & -4.4418 \\ 0.0050 & -3.9327 & 7.6052 \end{bmatrix}.$$

Simulation results are shown in Figs. 8–16 for Example 4.2. The state trajectories of the error system (10) are plotted in Figs. 8–10, illustrating the dynamics of synchronization error with SMC. We can see the time-varying delayed CDNs without the controller in Fig. 11. The closed-loop system with the various state responses is simulated in Figs. 12–14. Assume that the random initial values of the master system and the slave system in Figs. 12–14 are initially the responses of the states $x_{k1}(t) - \bar{x}_1(t)$, $x_{k2}(t) - \bar{x}_2(t)$ and $x_{k3}(t) - \bar{x}_3(t)$, where $(k = 1, 2, 3, 4, 5)$. It can

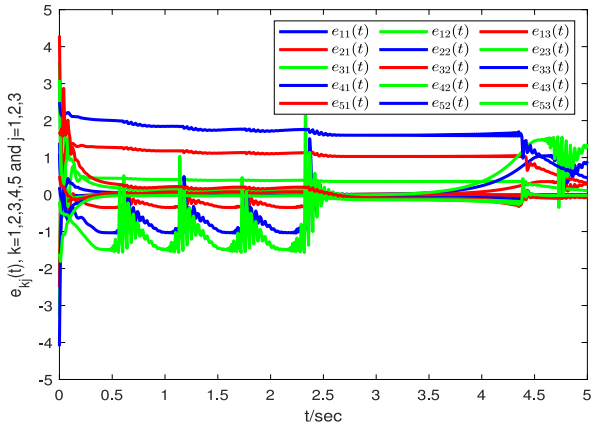

Fig. 11. Trajectories of error system (10) without control schemes.

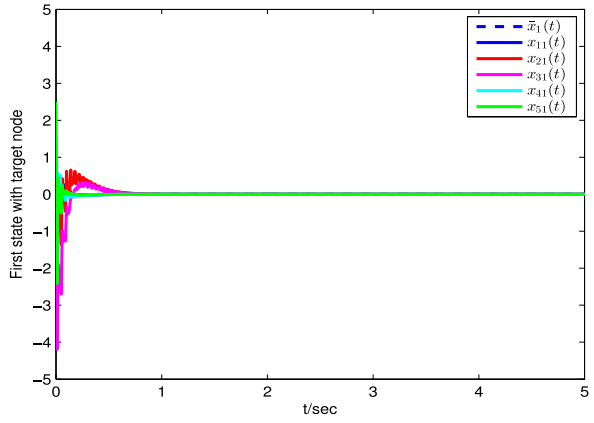

Fig. 12. State Response of $x_{k1}(t)$ $(k = 1, 2, 3, 4, 5)$ and $\bar{x}_1(t)$.

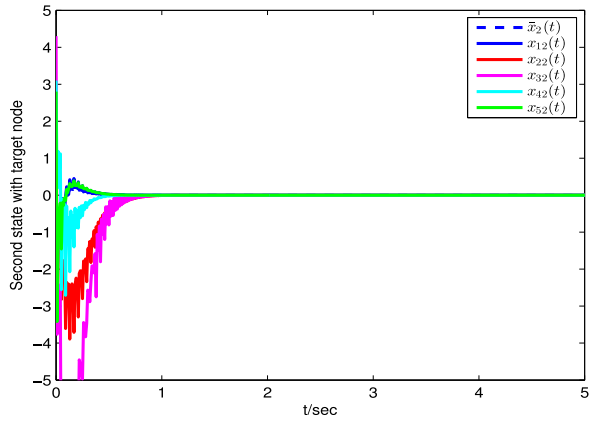

Fig. 13. State Response of $x_{k2}(t)$ $(k = 1, 2, 3, 4, 5)$ and $\bar{x}_2(t)$.

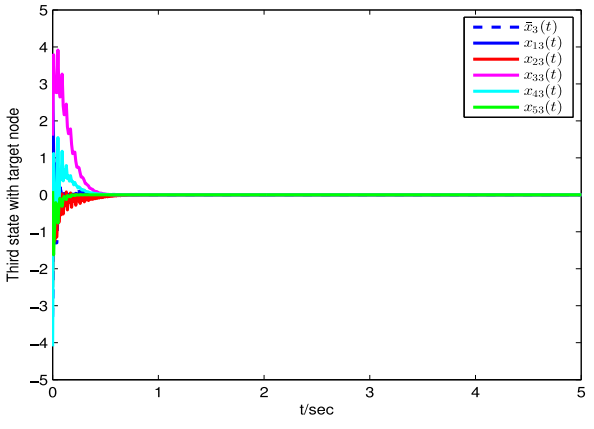

Fig. 14. State Response of $x_{k3}(t)$ $(k = 1, 2, 3, 4, 5)$ and $\bar{x}_3(t)$.

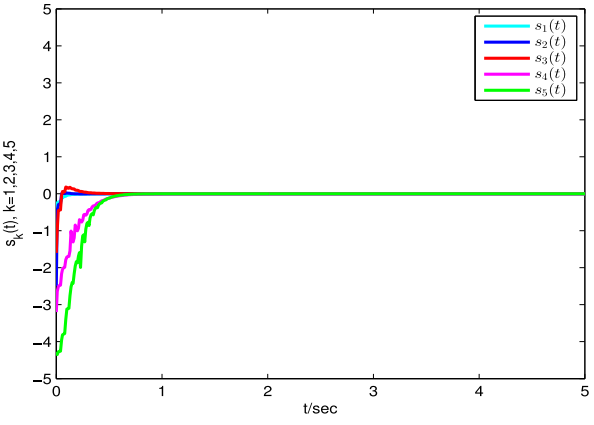

Fig. 15. Sliding mode surface function $s_k(t)$ for Example 4.2.

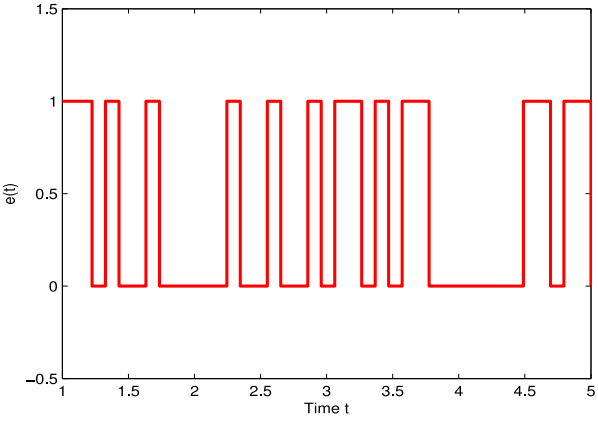

Fig. 16. Markovian jumping mode $r(t)$ for Example 4.2.

be clearly seen that the master and slave models are synchronized with the proposed control scheme. Moreover, Fig. 15 describes the trajectory of the sliding surface and shows that the sliding surface is continuous. Therefore, the systems (1) and (2) can successfully achieve exponential synchronization. Finally, Markov jump mode $r(t)$ is illustrated in Fig. 16.

In this example has been widely studied, thus we aim to give some comparisons on maximum allowable upper bounds of μ with the (Lee & Park, 2017; Li, Yuan, Fei, & Ding, 2018; Shi, Liu, Zhu, & Zhong, 2016; Zhang, Zeng, & Zhong, 2017). In Theorem 3.2, the MAUBs of μ can be computed out and listed in Table 2. To show the superiorities of our methods, we still use the theorems in Lee and Park (2017), Li et al. (2018), Shi et al. (2016), Zhang et al. (2017) to obtain the corresponding MAUBs, which can be illustrated in Table 2. From Table 2, it is clear that our results present much less conservatism than some existing ones. Especially, the NoDVs are also presented in Table 2.

Remark 4.1. The theoretical results presented in this article, which were validated using Examples 4.1 and 4.2, prove their effectiveness. A comparative analysis with (Zhang, Li, Yang, & Yan, 2015) is provided in Table 1, which highlights the advantages of our approach. In particular, our method based on Theorem 3.2 exhibits a higher

Table 1
Maximum allowable upper bounds (MAUBs) d for different μ.

μ	0	0.2	0.8	> 1
Zhang et al. (2015)	0.2529	0.2398	0.2365	0.2365
Theorem 3.2	1.7214	1.5642	1.3214	1.1021

Table 2
The MAUBs of μ for various methods and number of decision variables (NoDVs) in Example 2.

Utilized methods	MAUBs on μ	NoDVs
Theorem 3.1 (Shi et al., 2016)	0.4687	$21.5n^2 + 12.5n$
Theorem 1 (Zhang et al., 2017)	0.5185	$15.5n^2 + 8.5n$
Theorem 2 (Lee & Park, 2017)	0.5386	$47.5n^2 + 7.5n$
Theorem 1 (Li et al., 2018)	0.5584	$27.5n^2 + 15.5n$
Theorem 3.2	0.6000	$20.5n^2 + 9.5n$

upper bound on time-varying delays, leading to less conservative results compared to previous approaches. Consequently, the proposed method ensures lower computational complexity when dealing with the synchronization problem of complex dynamic networks under control.

Remark 4.2. The stability conditions presented in Theorem 3.2 are influenced by parameters including the scalars d and μ, and the known matrix $\mathcal{V}i$. These also includes positive definite matrices such as $\overline{P}_i$, $\overline{Q}_r$ $(r = 1, 2, 3, 4)$, $\overline{M}_l$, $\overline{N}_l$ $(l = 1, 2, \ldots, 5)$, $\overline{R}_a$, $\overline{R}_b$, $\overline{R}_1$, and any matrix Y_i of appropriate dimensions with $Y_i > 0$, together with the positive diagonal matrix Λ. These parameters are selected in a trial-and-error procedure to ensure the feasibility of the LMI-based conditions, in particular to achieve exponential synchronization of the system under consideration. However, the number of decision variables has a direct impact on the computational complexity. To solve this problem, an extended integral inequality from Lemma 2.3 is used to reduce the number of decision variables and thereby obtain less conservative constraints. With this approach, additional degrees of freedom are investigated, leading to simpler LMI structures and significantly reduced computational challenges.

5. Conclusion

In this work, the exponential synchronization problem in MJCDNs with time-varying delays using SMC strategies has been thoroughly investigated. By using a novel integral inequality lemma together with the LKF method and advanced analytical techniques, we have derived synchronization criteria formulated as LMIs. These criteria ensure the exponential synchronization of MJCDNs, which has been confirmed by extensive simulations. The proposed model and control design show significant results and robustness, making them applicable to a variety of complex network scenarios. The feasibility and applicability of the proposed technique have been demonstrated through the numerical simulation examples, which ensure that the proposed approach yields better results than the previous results (see Tables 1 and 2). The compilation of graphical representations demonstrates the effectiveness of the disclosed control strategy in maintaining the trajectory of the closed-loop system on the intended sliding surface. Moreover, the developed technique is applied to verify the feasibility of a practical model, namely Chua's circuit, which incorporates the Lur'e dynamical model. Therefore, our results have an important significance in theory as well as in practical applications of CDNs, including time delays. Future research will investigate fuzzy systems with distributed delays in chaotic environments with sliding mode controllers, filling a critical gap in current studies. In addition, optimizing network bandwidth by minimizing unnecessary data transmissions will be a focus. Given the increasing complexity and automation of attacks on neural networks, it is important to improve the resilience of control systems against such threats is imperative. These efforts aim to provide robust solutions for synchronization and stability in complex dynamic networks, contributing significantly to the field.

CRediT authorship contribution statement

Saravanan Shanmugam: Writing – original draft, Methodology, Formal analysis, Conceptualization. **Premraj Durairaj:** Writing – review & editing, Visualization, Software. **R. Vadivel:** Writing – review & editing, Visualization, Supervision, Methodology, Investigation. **Karthikeyan Rajagopal:** Validation, Supervision, Investigation, Formal analysis.

Declaration of competing interest

The authors declare that they have no known competing financial interests or personal relationships that could have appeared to influence the work reported in this paper.

Acknowledgments

The first Author S. Shanmugam would like to thank Easwari Engineering College, India, for their financial support, vide number SRM/EEC/RI/006.

Appendix

This appendix provides a detailed explanation of the operation of the infinitesimal operator $\mathcal{L}$ within the LKF (14) as $V(e_k(t), t, i)$. The infinitesimal operator $\mathcal{L}$ is defined as follows:

$$\mathcal{L}V(e_k(t), t, i) = \lim_{\Delta t \to 0} \frac{\mathbb{E}\{V(e(t+\Delta t), t+\Delta t, r(t+\Delta t))|e(t), t, i\} - V(e_k(t), t, i)}{\Delta t}$$
$$= V(e(t), t, i) + \dot{e}^T(t)V(e(t), t, i) + \sum_{j=1}^{S} \phi_{ij} V(e(t), t, j). \tag{43}$$

Proof. To find the expectation of the future value, we can written as follow,

$$\mathbb{E}\{V(e(t+\Delta t), t+\Delta t, r(t+\Delta t))|e(t), t, i\} \tag{44}$$

where, $t + \Delta t$ denoted as future time. By Definition 2.2 we can find the rate of change of V as Δt approaches zero as follows:

$$\lim_{\Delta t \to 0} \frac{\mathbb{E}\{V(e(t+\Delta t), t+\Delta t, r(t+\Delta t))|e(t), t, i\} - V(e_k(t), t, i)}{\Delta t}$$

From the above, we can get,

$$\mathcal{L}V(e_k(t), t, i) = V(e(t), t, i) + \dot{e}^T(t)V(e(t), t, i) + \sum_{j=1}^{S} \phi_{ij} V(e(t), t, j). \tag{45}$$

References

Akbari, N., Sadr, A., & Kazemy, A. (2020). Robust exponential synchronization of a Markovian jump complex dynamical network with piecewise homogeneous Markovian parameters. *IMA Journal of Mathematical Control and Information*, *37*(4), 1168–1191.

Ali, M. S., Yogambigai, J., Saravanan, S., & Elakkia, S. (2019). Stochastic stability of neutral-type Markovian-jumping BAM neural networks with time varying delays. *Journal of Computational and Applied Mathematics*, *349*, 142–156.

Chen, B., Niu, Y., & Zou, Y. (2013). Sliding mode control for stochastic Markovian jumping systems with incomplete transition rate. *IET Control Theory & Applications*, *7*(10), 1330–1338.

Chen, Y., Zhang, N., & Yang, J. (2023). A survey of recent advances on stability analysis, state estimation and synchronization control for neural networks. *Neurocomputing*, *515*, 26–36.

Ganesan, B., & Annamalai, M. (2023). Improved synchronization analysis via looped-Lyapunov for stochastic Markovian jump neural networks. *IEEE Transactions on Circuits and Systems II: Express Briefs*.

Guan, Z.-H., Liu, Z.-W., Feng, G., & Wang, Y.-W. (2010). Synchronization of complex dynamical networks with time-varying delays via impulsive distributed control. *IEEE Transactions on Circuits and Systems. I. Regular Papers*, *57*(8), 2182–2195.

Guo, L., Nian, X., Zhao, Y., & Duan, Z. (2012). Cluster synchronisation of Lur'e dynamical networks. *IET Control Theory & Applications*, *6*(16), 2499–2508.

He, Y., Wu, M., & She, J.-H. (2006). Delay-dependent exponential stability of delayed neural networks with time-varying delay. *IEEE Transactions on Circuits and Systems II: Express Briefs*, *53*(7), 553–557.

Hua, C., Wang, Y., & Wu, S. (2019). Stability analysis of neural networks with time-varying delay using a new augmented Lyapunov–Krasovskii functional. *Neurocomputing*, *332*, 1–9.

Karimi, H. R. (2012). A sliding mode approach to H_∞ synchronization of master-slave time-delay systems with Markovian jumping parameters and nonlinear uncertainties. *Journal of the Franklin Institute*, *349*(4), 1480–1496.

Lee, S. Y., Lee, W. I., & Park, P. (2018). Orthogonal-polynomials-based integral inequality and its applications to systems with additive time-varying delays. *Journal of the Franklin Institute*, *355*(1), 421–435.

Lee, T. H., & Park, J. H. (2017). Improved criteria for sampled-data synchronization of chaotic Lur'e systems using two new approaches. *Nonlinear Analysis. Hybrid Systems*, *24*, 132–145.

Li, Z., & Chen, G. (2006). Global synchronization and asymptotic stability of complex dynamical networks. *IEEE Transactions on Circuits and Systems II: Express Briefs*, *53*(1), 28–33.

Li, Q., Liu, X., Zhu, Q., Zhong, S., & Cheng, J. (2019). Stochastic synchronization of semi-Markovian jump chaotic Lur'e systems with packet dropouts subject to multiple sampling periods. *Journal of the Franklin Institute*, *356*(13), 6899–6925.

Li, T., Yuan, R., Fei, S., & Ding, Z. (2018). Sampled-data synchronization of chaotic Lur'e systems via an adaptive event-triggered approach. *Information Sciences*, *462*, 40–54.

Liu, M., Ho, D. W., & Shi, P. (2015). Adaptive fault-tolerant compensation control for Markovian jump systems with mismatched external disturbance. *Automatica*, *58*, 5–14.

Liu, X., Ma, G., Jiang, X., & Xi, H. (2016). H_∞ stochastic synchronization for master–slave semi-Markovian switching system via sliding mode control. *Complexity*, *21*(6), 430–441.

Lü, J., Yu, X., & Chen, G. (2004). Chaos synchronization of general complex dynamical networks. *Physica A. Statistical Mechanics and its Applications*, *334*(1–2), 281–302.

Mala, N., Vinodkumar, A., & Alzabut, J. (2023). Passivity analysis for Markovian jumping neutral type neural networks with leakage and mode-dependent delay. *AIMS Biophysics*, *10*(2), 184–204.

Mao, X. (1999). Stability of stochastic differential equations with Markovian switching. *Stochastic Processes and their Applications*, *79*(1), 45–67.

Peng, X., He, Y., Long, F., & Wu, M. (2020). Global exponential stability analysis of neural networks with a time-varying delay via some state-dependent zero equations. *Neurocomputing*, *399*, 1–7.

Rakkiyappan, R., Latha, V. P., & Sivaranjani, K. (2017). Exponential H_∞ synchronization of Lur'e complex dynamical networks using pinning sampled-data control. *Circuits, Systems, and Signal Processing*, *36*(10), 3958–3982.

Rakkiyappan, R., Sasirekha, R., Lakshmanan, S., & Lim, C. P. (2016). Synchronization of discrete-time Markovian jump complex dynamical networks with random delays via non-fragile control. *Journal of the Franklin Institute*, *353*(16), 4300–4329.

Rakkiyappan, R., Velmurugan, G., George, J. N., & Selvamani, R. (2017). Exponential synchronization of Lur'e complex dynamical networks with uncertain inner coupling and pinning impulsive control. *Applied Mathematics and Computation*, *307*, 217–231.

Sakthivel, R., Kwon, O., & Selvaraj, P. (2021). Observer-based synchronization of fractional-order Markovian jump multi-weighted complex dynamical networks subject to actuator faults. *Journal of the Franklin Institute*, *358*(9), 4602–4625.

Shanmugam, S., Rhaima, M., & Ghoudi, H. (2023). Exponential synchronization analysis for complex dynamical networks with hybrid delays and uncertainties under given control parameters. *AIMS Mathematics*, *8*, 28976–29007.

Shanmugam, S., Vadivel, R., & Gunasekaran, N. (2023). Finite-time synchronization of quantized Markovian-jump time-varying delayed neural networks via an event-triggered control scheme under actuator saturation. *Mathematics*, *11*(10), 2257.

Shi, K., Liu, X., Zhu, H., & Zhong, S. (2016). On designing stochastic sampled-data controller for master–slave synchronization of chaotic Lur'e system via a novel integral inequality. *Communications in Nonlinear Science and Numerical Simulation*, *34*, 165–184.

Sivaranjani, K., Rakkiyappan, R., & Joo, Y. H. (2018). Event triggered reliable synchronization of semi-Markovian jumping complex dynamical networks via generalized integral inequalities. *Journal of the Franklin Institute*, *355*(8), 3691–3716.

Tang, Z., Park, J. H., & Feng, J. (2018). Novel approaches to pin cluster synchronization on complex dynamical networks in Lur'e forms. *Communications in Nonlinear Science and Numerical Simulation*, *57*, 422–438.

Tang, Z., Park, J. H., & Zheng, W.-X. (2018). Distributed impulsive synchronization of Lur'e dynamical networks via parameter variation methods. *International Journal of Robust and Nonlinear Control*, *28*(3), 1001–1015.

Utkin, V. (1977). Variable structure systems with sliding modes. *IEEE Transactions on Automatic Control*, *22*(2), 212–222.

Wang, A., Dong, T., & Liao, X. (2016). Event-triggered synchronization strategy for complex dynamical networks with the Markovian switching topologies. *Neural Networks*, *74*, 52–57.

Wang, X., Liu, X., She, K., & Zhong, S. (2017). Pinning impulsive synchronization of complex dynamical networks with various time-varying delay sizes. *Nonlinear Analysis. Hybrid Systems*, *26*, 307–318.

Wang, J.-L., Wu, H.-N., & Huang, T. (2015). Passivity-based synchronization of a class of complex dynamical networks with time-varying delay. *Automatica*, *56*, 105–112.

Wu, Y., Li, H., & Li, W. (2019). Intermittent control strategy for synchronization analysis of time-varying complex dynamical networks. *IEEE Transactions on Systems, Man, and Cybernetics: Systems*, *51*(5), 3251–3262.

Xing, X., Yao, D., Lu, Q., & Li, X. (2015). Finite-time stability of Markovian jump neural networks with partly unknown transition probabilities. *Neurocomputing*, *159*, 282–287.

Xu, Z., Zhu, S., Liu, X., & Wen, S. (2023). Finite/fixed-time synchronization of nonidentical chaotic delayed neural networks with Markovian jump and uncertainties via sliding mode control. *International Journal of Robust and Nonlinear Control*, *33*(16), 10064–10082.

Yi, J.-W., Wang, Y.-W., Xiao, J.-W., & Huang, Y. (2013). Exponential synchronization of complex dynamical networks with Markovian jump parameters and stochastic delays and its application to multi-agent systems. *Communications in Nonlinear Science and Numerical Simulation*, *18*(5), 1175–1192.

Zhang, Y., Li, P., Yang, Q., & Yan, W. (2015). Synchronization criterion and control scheme for Lur'e type complex dynamical networks with switching topology and coupling time-varying delay. *Asian Journal of Control*, *17*(5), 1696–1706.

Zhang, R., Zeng, D., & Zhong, S. (2017). Novel master–slave synchronization criteria of chaotic Lur'e systems with time delays using sampled-data control. *Journal of the Franklin Institute*, *354*(12), 4930–4954.

Zhong, Y., & Song, D. (2023). Nonfragile synchronization control of T-S fuzzy Markovian jump complex dynamical networks. *Chaos, Solitons & Fractals*, *170*, Article 113342.

Zhou, J., & Chen, T. (2006). Synchronization in general complex delayed dynamical networks. *IEEE Transactions on Circuits and Systems. I. Regular Papers*, *53*(3), 733–744.